

UC Davis

UC Davis Previously Published Works

Title

Synaptic distributions of pS214-tau in rhesus monkey prefrontal cortex are associated with spine density, but not with cognitive decline

Permalink

<https://escholarship.org/uc/item/3d45x21g>

Journal

The Journal of Comparative Neurology, 527(4)

ISSN

1550-7149

Authors

Crimins, Johanna L
Puri, Rishi
Calakos, Katina C
[et al.](#)

Publication Date

2019-03-01

DOI

10.1002/cne.24576

Peer reviewed



Published in final edited form as:

J Comp Neurol. 2019 March 01; 527(4): 856–873. doi:10.1002/cne.24576.

Synaptic distributions of pS214-tau in rhesus monkey prefrontal cortex are associated with spine density, but not with cognitive decline

Johanna L. Crimins^{1,2}, Rishi Puri^{1,2}, Katina C. Calakos^{1,2}, Frank Yuk^{1,2}, William G. M. Janssen^{1,2}, Yuko Hara^{1,2}, Peter R. Rapp⁵, and John H. Morrison^{1,2,3,4,6,7}

¹Fishberg Department of Neuroscience and Kastor Neurobiology of Aging Laboratories Icahn School of Medicine at Mount Sinai, New York, NY 10029

²Friedman Brain Institute, Icahn School of Medicine at Mount Sinai, New York, NY 10029

³Department of Geriatrics and Palliative Medicine, Icahn School of Medicine at Mount Sinai, New York, NY 10029

⁴Graduate School of Biomedical Sciences, Icahn School of Medicine at Mount Sinai, New York, NY 10029

⁵National Institute on Aging, Laboratory of Behavioral Neuroscience, Baltimore, MD 21224

⁶California National Primate Research Center, Davis, CA 95616

⁷Department of Neurology, School of Medicine, University of California, Davis, CA 95616

Abstract

Female rhesus monkeys and women are subject to age- and menopause-related deficits in working memory, an executive function mediated by the dorsolateral prefrontal cortex (dlPFC). Long-term cyclic administration of 17 β -estradiol improves working memory, and restores highly plastic axospinous synapses within layer III dlPFC of aged ovariectomized monkeys. In this study, we tested the hypothesis that synaptic distributions of tau protein phosphorylated at serine 214 (pS214-tau) are altered with age or estradiol treatment, and couple to working memory performance. First, ovariectomized young and aged monkeys received vehicle or estradiol treatment, and were tested on the delayed response (DR) test of working memory. Serial section electron microscopic immunocytochemistry was then performed to quantitatively assess the subcellular synaptic distributions of pS214-tau. Overall, the majority of synapses contained pS214-tau immunogold particles, which were predominantly localized to the cytoplasm of axon terminals. pS214-tau was also abundant within synaptic and cytoplasmic domains of dendritic

Corresponding Author: John H. Morrison Ph.D., California National Primate Research Center, University of California at Davis, One Shields Avenue, Davis, CA 95616, jhmorrison@ucdavis.edu, Telephone: (530) 754-4829, Fax: (530) 754-6228.

Author Contributions:

Study conception and design: J.L.C., Y.H., P.R.R., J.H.M.

Acquisition of data: J.L.C., R.P., K.C.C., F.Y., W.G.M.J.

Analysis and interpretation of data: J.L.C., Y.H.

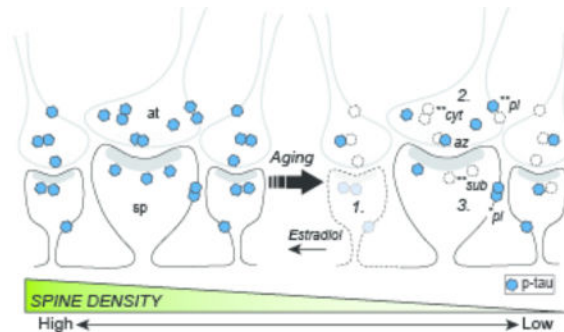
Drafting of manuscript: J.L.C., Y.H., J.H.M.

Critical revision of manuscript: J.L.C., K.C.C., Y.H., J.H.M., P.R.R.

Conflict of Interest Statement: The authors declare no competing financial interests.

spines. The density of pS214-tau immunogold within the active zone, cytoplasmic, and plasmalemmal domains of axon terminals, and subjacent to the postsynaptic density within the subsynaptic domains of dendritic spines, were each reduced with age. None of the variables examined were directly linked to cognitive status, but a high density of pS214-tau immunogold particles within presynaptic cytoplasmic and plasmalemmal domains, and within postsynaptic subsynaptic and plasmalemmal domains, accompanied high synapse density. Together, these data support a possible physiological, rather than pathological, role for pS214-tau in the modulation of synaptic morphology in monkey dIPFC.

GRAPHICAL ABSTRACT



Synaptic pS214-tau with aging and estradiol. (1) Estradiol restores small spines lost with age. (2) Axon terminal (at) pS214-tau is lost from the active zone (az), cytoplasmic (cyt), and plasmalemmal (pl) domains. (3) Spine (sp) pS214-tau is lost from the subsynaptic (sub) domain. Decreased pS214-tau correlates with synapse loss (asterisks).

Keywords

aging; Area 46; delayed response; estradiol; menopause; pS214; RRID:AB_2716719; RRID:AB_2750560; RRID:SCR_002865; RRID:SCR_014199

Introduction

Working memory is an executive function involving the transient, flexible storage of information “on-line” to guide reasoning and goal-directed behavior in the absence of external stimuli (Arnsten, Wang, & Paspalas, 2012; Goldman-Rakic, 1995). Loss of ovarian hormones during menopause exacerbates age-related working memory deficits in both humans and nonhuman primates (Bartus, Fleming, & Johnson, 1978; Hara, Waters, McEwen, & Morrison, 2015; Lacreuse, Mong, & Hara, 2015; Rapp & Amaral, 1989; Rapp, Morrison, & Roberts, 2003; Roberts, Gilardi, Lasley, & Rapp, 1997). Layer III pyramidal neurons in the dorsolateral prefrontal cortex (dIPFC) Area 46 promote working memory by engaging in recurrent excitation, and are highly vulnerable to the effects of aging and estrogen deprivation (Funahashi, Bruce, & Goldman-Rakic, 1989; Goldman-Rakic, 1995; Hara et al., 2015; Morrison & Baxter, 2012). We previously showed a dramatic loss of highly plastic dendritic spines from layer III dIPFC neurons, with a concomitant deficit in performance accuracy on a delayed response (DR) test of working memory in aged

ovariectomized (OVX) rhesus monkeys. Long-term cyclic administration of 17 β -estradiol abolished working memory impairment while increasing thin spine density (Crimins et al., 2017; Hao et al., 2007; P. R. Rapp et al., 2003). The precise molecular underpinnings of such synaptic and cognitive benefits of estradiol are not yet fully understood.

A major challenge in biomedical research is the development of new therapeutic approaches for Alzheimer's disease (AD), as rising incidence attributed to longer lifespan and aging—the highest risk factor for AD—increasingly burdens healthcare systems, caregivers, and individuals (Brookmeyer, Johnson, Ziegler-Graham, & Arrighi, 2007; Takizawa, Thompson, van Walsem, Faure, & Maier, 2015). The high failure rate of clinical trials in the face of enormous investment of resources and an active drugdevelopment pipeline further underscores the urgent need for novel approaches (Hung & Fu, 2017). Depleted estrogen, as initiated during the menopause transition, has long been suspected to contribute to the higher risk for AD and increased severity of cognitive symptoms documented in elderly women compared to men (Andersen et al., 1999; Laws, Irvine, & Gale, 2016; Pike, 2017; Ruitenber, Ott, van Swieten, Hofman, & Breteler, 2001). Dementia risk is also significantly increased in women who have undergone either premature or surgical menopause (by oophorectomy and or/hysterectomy), further implicating low hormone levels in disease etiology (Bove et al., 2014; Phung et al., 2010; Rocca et al., 2007; Rocca, Grossardt, & Shuster, 2011; Ryan et al., 2014). However, profound disparities between positive basic research findings in animal models and observational data in women, versus adverse outcomes in early clinical trials where an increased risk for dementia and poorer cognitive performance was seen in older postmenopausal women receiving hormone treatment, elicited early skepticism surrounding hormone replacement therapy as a tool for reducing AD-risk and ameliorating cognitive deficits (Brinton, 2009; Hara et al., 2015; S. R. Rapp et al., 2003; Shumaker et al., 2004; Shumaker et al., 2003). Later studies, however, reported reduced AD risk in women treated at, or soon after, menopause onset, supporting a critical window for treatment success (Henderson et al., 2005; Shao et al., 2012; Whitmer, Quesenberry, Zhou, & Yaffe, 2011). Still, the Kronos Early Estrogen Prevention Study Cognitive and Affective Study (KEEPS-Cog trial), the largest and most recent trial to test cognitive outcomes of hormone therapy in post-menopausal women, failed to demonstrate any cognitive benefit, despite evidence for positive effects of transdermal estradiol on AD-related brain pathology and dlPFC volume (Gleason et al., 2015; Kantarci et al., 2016; Kantarci et al., 2018). Hence, whether hormone replacement therapy may be a viable intervention for AD or cognitive impairment in women remains equivocal.

From a neuroanatomical viewpoint, the same brain circuits that undergo synaptic collapse during cognitive aging and menopause are also highly vulnerable to the effects of AD-related pathology, and ultimately degenerate and die over the time course of the disease (Hara, Rapp, & Morrison, 2012; Hara et al., 2015; Morrison & Baxter, 2012; Morrison & Hof, 2002). Estrogens' neuroprotective activity, e.g., targeting synaptotoxicity and amyloid- β (A β) central to AD development, has been a major focal point over decades of research (Brinton, 2009; Merlo, Spampinato, & Sortino, 2017). Application of combined genetic AD and estrogen deficiency rodent models have been particularly instrumental in revealing a possible role for estrogen in reducing A β pathology (Merlo et al., 2017). Yet, of the many treatments shown to clear A β pathology in transgenic models, it is worth bearing in mind

that none have proven clinically useful (Hung & Fu, 2017). Of emerging interest has been the involvement of estrogens in mechanisms pertinent to hyperphosphorylated tau protein, the principal proteinaceous component of neurofibrillary tangle (NFT) pathology that accumulates in degenerating neurons and correlates with cognitive decline in AD patients (Arriagada, Growdon, Hedley-Whyte, & Hyman, 1992; Giannakopoulos et al., 2003; Gomez-Isla et al., 1997; Grundke-Iqbal et al., 1986). In advanced stages of late-onset AD, explicit dementia accompanies extensive neurodegeneration and tau pathology in association cortices, including the dlPFC, where pyramidal neuron connections relevant to higher-order cognition are severely afflicted (Braak, Alafuzoff, Arzberger, Kretschmar, & Del Tredici, 2006; Braak & Braak, 1995; Braak, Thal, Ghebremedhin, & Del Tredici, 2011; Nelson et al., 2012). *In vitro* experiments suggest that estradiol may attenuate or prevent AD-like tau hyperphosphorylation, but whether a parallel mechanism exists in the dlPFC is unknown (Alvarez-de-la-Rosa et al., 2005; X. A. Liu et al., 2008; Shi et al., 2008; Zhang & Simpkins, 2010).

A high level of tau phosphorylated at serine 214 (pS214-tau) accumulates in AD brain, and was recently documented within layer III dlPFC dendritic spines of aged, surgically intact rhesus monkeys susceptible to compromised dlPFC network function, and poor working memory performance (Augustinack, Schneider, Mandelkow, & Hyman, 2002; Carlyle et al., 2014; Jicha et al., 1999; Paspalas et al., 2017). Though synaptic ptau was qualitatively extensive, tau fibrillation was sporadic, and was identified only in dlPFC from the very oldest monkeys. Paired with significant spine loss observed in dlPFC of cognitively impaired aged monkeys by our own group, evidence of synaptic ptau reactivity in the absence of prevalent fibrillar pathology and neuron death may be suggestive of early synaptic dysfunction in AD (Dumitriu et al., 2010; Hao et al., 2007). Importantly, estrogen may reduce abnormal phosphorylation of tau by kinases, including cAMP-dependent protein kinase (PKA) principally responsible for generating pS214-tau (Alvarez-de-la-Rosa et al., 2005; Goodenough, Schleusner, Pietrzik, Skutella, & Behl, 2005; Jicha et al., 1999; X. A. Liu et al., 2008). Thus, harnessing a possible relationship between estrogen and synaptic pS214-tau in aging dlPFC could offer a powerful future strategy to support synaptic health, and dlPFC-dependent cognition.

Might cyclic estradiol treatment of aged OVX rhesus monkeys rescue vulnerable layer III dlPFC spines and improve working memory by modulating synaptic pS214-tau? Here we test the possibility that subcellular distributions of pS214-tau in axospinous dlPFC synapses in aged OVX monkeys from our initial preclinical studies are altered with cyclic 17 β -estradiol treatment, and couple to dlPFC-dependent working memory. Our data reveal an age-dependent reduction in the density of pS214-tau within presynaptic and postsynaptic domains, which correlate with synapse loss. This work suggests that pS214-tau may support, rather than compromise, synaptic integrity in rhesus monkey dlPFC, and highlights a potential difference in age- and AD-reliant processes in dlPFC synapses from humans versus nonhuman primates.

Materials and Methods

Subjects

A total of eight young adult (9.885 ± 0.733 years old, mean \pm SEM) and 8 aged (25.240 ± 0.944 years old) female rhesus monkeys (*Macaca mulatta*) were used in the present study. Monkeys were sacrificed as part of a larger cohort from earlier experiments, each designed to probe the effects of age, surgical menopause, and estradiol replacement on cognition and diverse neurobiological measures (Crimins et al., 2017; Hao et al., 2007; Hao et al., 2006; Hara et al., 2016; P. R. Rapp et al., 2003; A. C. Wang, Hara, Janssen, Rapp, & Morrison, 2010; Yague et al., 2008). Thus, behavioral characterization of monkeys included in this study has been previously reported (Hao et al., 2007; P. R. Rapp et al., 2003). Monkeys were singly housed in colonies of ~40 individuals at the California National Primate Research Center, University of California, Davis. Water was available *ad libitum* in the home cage, and monkey chow was given daily following behavioral testing, and was routinely supplemented with fresh fruit. All experiments were conducted in compliance with the National Institutes of Health *Guide for the Care and Use of Laboratory Animals* and were approved by the Institutional Animal Care and Use Committee at the University of California, Davis.

Rhesus macaques as a model for aging and menopause

Rhesus macaques are highly valuable models of human aging and menopause for a number of critical reasons. Like humans, they exhibit age- and menopause-related cognitive decline, which can be quantified over the lifespan using a battery of cognitive tests. Tests used in rhesus monkeys are similar to, if not the same as, those used to assess cognitive status in humans (Nagahara, Bernot, & Tuszyński, 2010; Squire, Zola-Morgan, & Chen, 1988). Brain anatomy, neuronal gene expression, reproductive physiology, and progression of endocrine senescence of rhesus macaques are also similar to those of humans (Gill, Sharpless, Rado, & Hall, 2002; Hara, Rapp, et al., 2012;

Loerch et al., 2008; Matt, Kauma, Pincus, Veldhuis, & Evans, 1998; Nichols et al., 2005; Petrides & Pandya, 1999; Walker & Herndon, 2008; Woller et al., 2002). Though relatively later in life, rhesus monkeys undergo a low-estrogen menopause that is qualitatively similar to that in women (Gilardi, Shideler, Valverde, Roberts, & Lasley, 1997; Nichols et al., 2005; Walker & Herndon, 2008). The lifetime of a rhesus monkey is ~35 years, and the ratio to human age is roughly 1:3 (Tigges, Gordon, McClure, Hall, & Peters, 1988). Lastly, rhesus monkeys do not develop full-blown AD pathology, so the effects of age- and menopause-related processes on neurobiological parameters can be studied in the absence of neuroanatomical hallmarks of the disease, including extensive NFT deposition and large-scale neuron death (Finch & Austad, 2015; Gearing, Tigges, Mori, & Mirra, 1996; Peters & Morrison, 1999; Sloane et al., 1997).

Ovariectomy and 17 β -estradiol replacement

Prior to behavioral testing, all monkeys received bilateral ovariectomies, and were randomly assigned to vehicle or estradiol treatment groups, as described in detail previously (P. R. Rapp et al., 2003). Monkeys were sedated with ketamine (10 mg/kg, i.m) and atropine (0.04

mg/kg, s.c.), and anesthetized with isoflurane. The ovarian vessels and fallopian tubes were isolated, ligated, and severed via a ventral midline incision. The ovaries were then extracted, and the incision closed. Monkeys were monitored until responsive, and oxymorphone was administered (1.5 mg/kg) 3 times/day over 2 days. Following a post ovariectomy period of ~30 weeks, monkeys in the young and aged estradiol (E) treatment groups (young-E, n=3; aged-E, n= 4 monkeys) were injected with 100 µg of estradiol cypionate (Pharmacia) in 1 mL of sterile peanut oil (i.m.) every 21 days. Monkeys in the vehicle (V) treatment groups (young-V, n=5; aged-V, n=4 monkeys) were injected with an equivalent volume of peanut oil according to the same schedule. Treatment extended over 2–3 years of behavioral testing. Injections were administered in a blinded fashion.

Behavioral testing

The Delayed Response (DR) test of visuospatial working memory was conducted as previously described (P. R. Rapp et al., 2003). Monkeys watched from behind a transparent screen while either the left or the right recessed well of a test tray was baited with a food reward. Both wells were then covered with identical plaques, and an opaque screen was lowered to block the test tray from view for a given delay (or, retention) interval. Finally, both screens were lifted, and contingent upon correct selection of the baited well, the subject was permitted to retrieve the food reward by displacing the plaque. During the acquisition phase, the delay interval was first set to 0-s. After a performance criterion of 90% correct was met, a second 1-s delay interval was implemented until criterion was again achieved; the number of trials required to meet criterion (trials to criterion, TTC) were recorded for each subject during this phase. Following task acquisition, working memory was taxed with increasingly longer delays of 5-, 10-, 15-, 30-, and 60-s during the testing phase. Each delay interval was tested for a total of 90 trials (30 trials/day; inter-trial interval = 20-s), and for each delay interval, the percentage of correct responses (*i.e.* performance accuracy) was calculated for each subject. DR acquisition and performance accuracy data for each subject are presented in Table 1.

Perfusion and tissue processing for electron microscopy

Monkeys were sacrificed upon completion of behavioral testing, and 24 h following the last administration of vehicle or estradiol. Monkeys were first tranquilized with ketamine hydrochloride (25 mg/kg), and then deeply anesthetized with pentobarbital (20–35 mg/kg, i.v.); afterward, they were intubated, and mechanically ventilated. A thoracotomy was performed and 1.5 ml of 0.5% sodium nitrate was injected into the left ventricle of the heart. The descending aorta was clamped and monkeys were sacrificed by exsanguination while being perfused transcardially with ice cold 1% paraformaldehyde (PFA) in 0.1M phosphate buffer (PB, pH 7.2) for 1 min, followed by 4% PFA/PB with 0.125% glutaraldehyde for 12 min. A frontal block containing the PFC region that spans the sulcus principalis (Brodmann's Area 46) was postfixed in 4% PFA/PB with 0.125% glutaraldehyde for 6 h, and briefly rinsed in PB. The block was then cut with a vibrating microtome (Leica) into 400 µm-thick sections for subsequent freeze substitution and embedding.

Freeze substitution and low-temperature resin embedding of sections were performed as previously described (Crimins et al., 2017; A. C. Wang et al., 2010). Briefly, after

cryoprotection in increasing concentrations of glycerol, sections were plunged into liquid nitrogen-cooled liquid propane (-190°C) in a Universal Cryofixation System KF80 (Reichert-Jung). Then, they were immersed in 1.5% uranyl acetate in anhydrous methanol at -90°C for 24 h in a Cryosubstitution Automatic Freeze Substitution System (Leica); the temperature was then raised by increments of $4^{\circ}\text{C}/\text{h}$ to 45°C . Sections were briefly rinsed with anhydrous methanol, and infiltrated with increasing concentrations of Lowicryl HM20 resin (Electron Microscopy Sciences) for 1 h each at -45°C ; this was followed by a single overnight incubation in pure resin. The resin was polymerized using Ultraviolet light (360 nm) first at -45°C for 48h, and then at room temperature for an additional 48h. Five or more consecutive ultrathin 80 nm-thick sections were cut using a Diatome diamond knife (Electron Microscopy Sciences), and then mounted on a formvar-supported slot grid (Electron Microscopy Sciences).

Primary antibody

The mouse monoclonal (IgM) antibody raised against human tau protein phosphorylated at serine 214 (CP3) was kindly provided by Dr. Peter Davies (P. Davies, Albert Einstein College of Medicine, New York, USA; Cat# CP3, RRID:AB_2716719) for use in this study (Jicha et al., 1999). This highly specific and well-characterized antibody was generated by immunizing mice with affinity-purified paired helical filaments (PHFs) prepared from human AD brain, the major fibrillar constituent of NFT pathology central to AD (Grundke-Iqbal et al., 1986; Jicha et al., 1999). For initial characterization experiments, Jicha et al. (1999) used western blot to show high levels of CP3 reactivity in PHF preparations, but not in adult rat, fetal or adult mouse, or fetal or adult human control brain homogenates (Jicha et al., 1999). Specific CP3 detection of PKA-dependent phosphorylation of recombinant tau at S214, but not at sites targeted by alternative kinases, was confirmed by the same method. Further, CP3-positive NFT pathology in AD hippocampus was demonstrated at the light level using immunostaining approaches. CP3 also reacted with synthetic pS214-tau peptide, but not with a panel of other tau peptides by ELISA. Several other groups have since extensively used the CP3 antibody to demonstrate p-tau-dependent pathology in human AD, and in transgenic AD mouse model brain by western blot and immunohistochemical methods (Allen et al., 2002; Augustinack et al., 2002; Lewis et al., 2001; Lewis et al., 2000; Vingtdeux, Davies, Dickson, & Marambaud, 2011). Immunohistochemical evaluation of human AD brain showed that elevated CP3 paralleled pronounced dendritic atrophy. CP3 immunoreactive intra- and extra-neuronal NFTs were also visible in the same tissue (Augustinack et al., 2002). Carlyle and colleagues (2014) performed electron microscopic immunocytochemical experiments with the CP3 antibody, providing the first demonstration of pS214-tau in aged rhesus monkey PFC (Carlyle et al., 2014). In a recent follow-up study using both light and electron microscopy, the same group replicated these qualitative findings, and extended their observations to include entorhinal cortex (Paspalas et al., 2017). Immunogold particles were localized to both presynaptic and postsynaptic sites within PFC axospinous synapses, in agreement with observations forming the basis for the present study. In the present study, antibody specificity was confirmed by a peptide adsorption control experiment using a commercially available peptide (sc-12413 P; Santa Cruz Biotechnology, Inc.) in which no immunogold labeling was observed. In addition, CP3 detected mature NFTs and neuropil threads in human AD brain, but not in healthy control brain visualized by

immunofluorescence microscopy (data not shown). Finally, CP3 produced immunogold labeling patterns similar to another well-characterized, and phosphorylation dependent tau antibody routinely used to detect tau pathology in human AD brain (Braak et al., 2006; Braak & Braak, 1995).

Postembedding immunogold labeling

To eliminate excess aldehydes, sections were first treated with 0.1% sodium borohydride and 50 mM glycine, and then washed with 0.3% NaCl/0.005 M Tris buffered saline TBS. Sections were subsequently incubated in 2% human serum albumin (HSA) in TBS for 30 min at room temperature to block nonspecific binding of antisera. Following blocking, they were incubated overnight in a primary antibody in a solution of anti-pS214-tau (CP3; 1:25 dilution; Dr. Peter Davies) in 2% HSA/TBS. After an additional TBS wash, and blocking with 2% HSA/TBS, sections were incubated with goat antimouse IgM (μ -chain) conjugated to 10 nm gold particles (1:20 dilution; Electron Microscopy Sciences, Cat# 25149, RRID:AB_2750560) in 2% HSA with 5 mg/mL polyethylene glycol in TBS. After a final TBS wash, sections were dried before counterstaining with 1% uranyl acetate in distilled water for 45 min. To confirm specificity of the secondary antibody, the absence of gold particles was verified when the primary antibody was omitted from the experiment.

Quantitative analysis of pS214-tau immunolabeling

Experimenters blinded to group designation, and to behavioral performance of monkeys carried out all electron microscopy imaging, and characterization of synapses. Electron micrographs were acquired at 75 kV with a Hitachi H-7700 electron microscope (Hitachi High Technologies) equipped with an AMT Advantage CCD camera. For each monkey, at least 25 image sets of 5 serial ultrathin sections were captured at 6,000x magnification; the minimum target number of postsynaptic densities (PSDs) captured per field of view was set to 5. To ensure unequivocal sampling from Layer III Area 46, images were obtained from 230–350 μ m deep to the basal laminar aspect of Layer I. Electron micrographs were adjusted for brightness, contrast, and sharpness using Adobe Photoshop (version CS5, RRID:SCR_014199).

As with our previous work, the synapse-sampling scheme used here was designed to obtain the maximum amount of highly accurate immunolabeling and synaptic morphological information per synapse across a very large population of synapses (Crimins et al., 2017; Hara, Punsoni, et al., 2012). To meet this objective, the middle (third) section was used as a reference section, and each synapse with a visible PSD in this section was marked and followed across the 5 serial sections for inclusion in the dataset. Over 2,200 synapses (range, 131–148 synapses/monkey) were marked for subsequent morphological and immunolabeling analyses. The total volume of dIPFC layer III assessed averaged 312 μ m³ per monkey (range, 297–357 μ m³/monkey). Areal density was defined as the number of synapses marked in each reference section expressed as a function of the summed total image area. This calculation allowed for accurate assessment of the relative change in synapse density between groups (despite that absolute values may differ), and enabled time efficient, maximization of sampling across monkeys. Synapse density values were previously reported as part of a recent systematic-random, serial immunoelectron study by

Crimins et al. (2017) in which distributions of an estrogen receptor in layer III dIPFC axospinous synapses were characterized in a larger cohort of monkeys, including the smaller subset used here (Crimins et al., 2017). Importantly, synapse density data reported here closely correlated with our previous spine density estimates (see Hao et al., 2007 for details) in individual Lucifer-yellow filled layer III dIPFC neurons from the same monkeys (Pearson's correlation; $n = 16$ monkeys, $r = 0.631$, $p = 0.015$), and with values determined using the size-frequency method suggested by Colonnier and Beaulieu (1985) often used in single section studies (Pearson's correlation, $n = 16$ monkeys, $r = 0.925$, $p = 2.874 \times 10^{-7}$) (Colonnier & Beaulieu, 1985). The latter method was chosen to cross validate our own findings because it was employed by Peters and colleagues (2008) to first describe the age-related loss of synapses in rhesus monkey PFC at the ultrastructural level (Peters, Sethares, & Luebke, 2008). Together, these strong positive relationships confirm accurate representation here of the previously established convergent effects of age and estrogen on spine density in monkey layer III dIPFC.

Synapse morphology was evaluated as previously described in detail (Crimins et al., 2017; Hara, Punsoni, et al., 2012). Briefly, synapses were categorized as perforated when a discontinuity in the PSD was visible in any one of the 5 serial sections; all other synapses were marked as non-perforated. Synapses containing one or more gold particles within the presynaptic or postsynaptic compartment, or within the synaptic cleft were considered labeled. The synapse was classified as unlabeled when gold particles were entirely absent from the synaptic complex. All measurements were obtained using tools available in Adobe Photoshop (CS5). Briefly, axon terminal and spine head diameters were determined at their maximum width oriented parallel to the synaptic cleft. As with our previous work, the volume and surface area of each axon terminal and spine were estimated using these diameters to calculate the volume and surface area of a sphere and half sphere, respectively (Crimins et al., 2017; Hara, Punsoni, et al., 2012). To estimate synaptic, subsynaptic and active zone areas, the lengths of PSD segments measured across the five consecutive serial images were summed and multiplied by section thickness (80 nm). The lasso tool was used to measure the area of presynaptic mitochondrial profiles in each of the five sections.

Using the same criteria as described in our previous work, immunogold particles localized to each labeled synapse were assigned to one of 4 presynaptic, or 4 postsynaptic domains according to their precise location within the synapse (Crimins et al., 2017; Hara, Punsoni, et al., 2012). These 8 synaptic "bins" were named, and defined as follows: (1) the presynaptic active zone bin consisted of the area within 30 nm of the presynaptic membrane that was directly apposed to the spine PSD; (2) the presynaptic plasmalemmal bin was defined as the area within 30 nm of the plasma membrane, but outside the presynaptic active zone; (3) the presynaptic cytoplasmic bin consisted of the axon terminal core more than 30 nm from the plasma membrane, outside the active zone bin, and also excluding mitochondria; (4) the presynaptic mitochondrial bin included the area within 30 nm of the mitochondrial outer membrane, within the mitochondrial core, and on sections adjacent to those containing the last visible mitochondrion; (5) the synaptic bin consisted of the PSD within 30 nm of the postsynaptic membrane, the synaptic cleft, and the perisynaptic zone; this zone included two regions, each 30 nm lateral to the PSD within 30 nm of the plasma membrane, and on adjacent sections to the last visible PSD; (6) the subsynaptic bin was

defined as the area directly subjacent to the PSD, within 60 nm of the plasma membrane; (7) the plasmalemmal bin was comprised of the area within 30 nm of the plasma membrane, but outside the synaptic bin; and, (8) the cytoplasmic bin included the core of the spine head outside all other postsynaptic domains.

Statistical analyses

IBM SPSS Statistics software version 20 (IBM Corporation, RRID:SCR_002865) was used to perform all statistical analyses. A one-sample Kolmogorov-Smirnov test confirmed that behavioral and synaptic data followed a normal distribution ($p > 0.05$ for all) and parametric tests were used accordingly. Two-way multivariate ANOVA was used to examine age and treatment effects. One-way ANOVA followed by Tukey's post hoc test was used to assess between-group differences across the four groups (young-V, young-E, aged-V, aged-E), while correcting for multiple comparisons. Observed power was determined using ANOVA, and confirmed sufficient sample size to support the data. Pearson's product moment correlation was used to evaluate relationships between cognitive and synaptic indices. Due to the risk of over-correction, correlations were not corrected for multiple comparisons. The significance level was set to $p = 0.05$, and all data are reported as mean \pm SEM. To avoid inflation of statistical power, group means were calculated using one average value for each monkey, rather than using each individual synapse as n .

Results

Behavioral characterization

Behavioral data for the subset of 16 monkeys available for inclusion in the present study have been described in detail elsewhere (Crimins et al., 2017; Hao et al., 2007; Hara et al., 2016; P. R. Rapp et al., 2003; A. C. Wang et al., 2010). Group average delayed response (DR) task acquisition and performance accuracy data are listed in Table 1. Briefly, there were no significant age or treatment effects on the number of trials required to meet task acquisition criterion of 90% correct at either the 0-s or 1-s retention interval ($p > 0.05$). This finding is in agreement with reports that aged and menopausal monkeys do not typically exhibit deficits during task acquisition, and tend to perform well at very short delay intervals (Rapp & Amaral, 1989; P. R. Rapp et al., 2003). When working memory was challenged with increasingly longer delay intervals (5–60-s), a repeated-measures ANOVA showed a significant effect of delay on average performance accuracy ($F_{(3,48)} = 12.636$, $p = 4.233 \times 10^{-7}$, observed power = 1.00). Despite the absence of a group effect, and of a group \times delay interval interaction ($p > 0.05$ for both), the aged-V group performed on average numerically worse than the young-V, young-E, and aged-V groups at each delay interval apart from 5-s; this is consistent with our previous observations in a larger cohort of monkeys, which included those used here (Hao et al., 2007; P. R. Rapp et al., 2003). In contrast, the aged-E group in the present study, as before, performed at levels similar to those of young-V and young-E monkeys, providing support for the beneficial effects of cyclic estradiol replacement on working memory in aged, but not in young, monkeys (Hara et al., 2015; P. R. Rapp et al., 2003; Voytko, 2000). Importantly, for the purposes of this study, that behavioral and synaptic morphological and immunolabeling data were obtained

from the same monkeys allowed for invaluable probing of the potential linkage between neurobiological measures, and individual differences in DR performance accuracy.

Morphological characteristics of synapses examined

We previously demonstrated a significant age-related increase in dendritic spine size in individual Lucifer yellow-filled layer III Area 46 pyramidal neurons from the same monkeys used in this study (Hao et al., 2007). To confirm these findings at the electron microscopic level using an anatomical index of both synaptic contact size and efficacy, PSD length was measured for each synapse (Harris & Stevens, 1989). In agreement with our earlier work, a two-way ANOVA demonstrated a significant main effect of age, but not of treatment, such that average PSD length was significantly longer in synapses from aged versus young monkeys ($F_{(1,12)} = 12.073$, $p = 0.005$, observed power = 0.89; Fig. 1, **left**). Tukey's post hoc test revealed that the aged-E group had a significantly longer average PSD length than the young-E group ($p = 0.047$).

Alterations in axonal/presynaptic terminal morphology (*e.g.* swelling) in aged monkey prefrontal cortex have been previously shown at both the light and electron microscopic levels (Cork, Masters, Beyreuther, & Price, 1990; Peters & Sethares, 2002). Strong evidence also indicates that estrogen can exert a variety of actions on the patterns of connectivity and metabolic integrity of monkey Area 46 presynaptic terminals (Hara et al., 2014, 2016). In the present study, the diameter of each axon terminal was measured to evaluate the possible effects of age and estrogen on axon terminal size that might accompany changes in dendritic spine size. Two-way ANOVA showed a significant main effect of age ($F_{(1,12)} = 33.106$, $p = 9.10 \times 10^{-5}$, observed power = 1.00), and of treatment ($F_{(1,12)} = 4.942$, $p = 0.046$, observed power = 0.533), on axon terminal diameter (Fig. 1, **middle**). Tukey's post hoc tests revealed that the average axon terminal diameter of synapses from aged monkeys was significantly longer than those of young-V monkeys, independent of treatment group (aged-V vs. young-V, $p = 0.003$; aged-E vs. young-V, $p = 2.93 \times 10^{-4}$). Average axon terminal diameter was also significantly longer in synapses from Aged-E versus Young-E monkeys ($p = 0.018$).

Indices of dendritic spine size and efficacy are typically directly proportional to those of corresponding presynaptic inputs. For instance, the size of the PSD correlates with the number of postsynaptic receptors, and the number of presynaptic vesicles, including those sequestered within the readily releasable pool (Arellano, BenavidesPiccione, Defelipe, & Yuste, 2007; Harris & Stevens, 1988, 1989; Lisman & Harris, 1993; Pierce & Lewin, 1994; Yeow & Peterson, 1991). Indeed, structural rearrangements of a given dendritic spine can be used to predict concomitant alterations to the presynaptic element, and vice versa (Harris & Stevens, 1988, 1989; Lisman & Harris, 1993). A bivariate Pearson's analysis was used to test for the potential relationship between dendritic spine and axon terminal size. A positive relationship emerged between average PSD length and axon terminal diameter ($n = 16$ monkeys, $r = 0.760$, $p = 0.001$; Fig. 1, **right**).

Distributions of synaptic pS214-tau

Pre- and postsynaptic localizations of pathological tau species have been previously documented in aged monkey forebrain, and the presence of p-tau in Area 46 of young

monkeys has also been recently described (Carlyle et al., 2014; Hartig et al., 2000; Oikawa, Kimura, & Yanagisawa, 2010; Paspalas et al., 2017). Here, the majority of axon terminals (~90%) and dendritic spines (~85%) contained p-tau immunogold particles. Thus, in most instances (~77% of synapses), p-tau immunogold particles were localized to both pre and postsynaptic compartments of the same synaptic complex. The percentage of synapses containing p-tau did not differ with age or estradiol treatment, and was similar across all 4 groups of monkeys (multivariate ANOVA, $p > 0.05$; data not shown). This was also the case when smaller-type non-perforated and larger-type perforated synapse spines were examined separately (>95% of each type contained ptau immunogold particles), indicating that p-tau localizes to both highly plastic and stable synaptic subclasses regardless of age or hormone status (multivariate ANOVA, $p > 0.05$; data not shown).

To examine subcellular distributions of p-tau, each immunogold particle was assigned to one of 4 presynaptic, or 4 postsynaptic, domains (or, “bins”) based on its location within an individual synapse followed across 5 serial ultrathin sections (Fig. 2a,b). First, relative frequencies of p-tau were calculated by dividing the number of immunogold particles in each synaptic bin by the sum total number of immunogold particles averaged for each monkey to determine whether overall synaptic distribution patterns were altered with aging or estrogen. No significant age or treatment effects were present for any relative frequency parameter, and all values were similar across all 4 groups of monkeys ($p > 0.05$ for all; data not shown). However, more than one-third of all p-tau immunogold particles were distributed to the axonal cytoplasmic bin (Fig. 2c), consistent with its predominate enrichment in axons and principal role in binding and stabilizing microtubules, (Black, Slaughter, Moshia, Obrocka, & Fischer, 1996; Kempf, Clement, Faissner, Lee, & Brandt, 1996; Weingarten, Lockwood, Hwo, & Kirschner, 1975). Presynaptic active zone, mitochondrial, and plasmalemmal domains each contained ~5–8% of p-tau immunogold particles. Similar to patterns of synaptic distributions of pS214-tau observed by others, and favoring roles for tau in mediating interactions between N-methyl-D-aspartate (NMDA) receptors and the PSD, and in feedforward calcium signaling, p-tau was also relatively abundant within the synaptic and cytoplasmic domains of dendritic spines (Carlyle et al., 2014; Frandemiche et al., 2014; L. M. Ittner et al., 2010; Mondragon-Rodriguez et al., 2012; Paspalas et al., 2017; Roberson et al., 2011; Salter & Kalia, 2004). In addition, it was often observed at the spine apparatus, as well as other endomembranous structures across the synaptic complex, consistent with earlier reports (Carlyle et al., 2014; Paspalas et al., 2017; data not shown). Dendritic spine subsynaptic and plasmalemmal bins each contained ~6% of p-tau immunogold particles; the localization of tau within these domains supports its proposed interactions with multiple different signaling molecules, the actin cytoskeleton, and the lipid-rich domains such as the plasma membrane (Y. Wang & Mandelkow, 2016).

Since the size of the synaptic complex could potentially confound the number of immunogold particles localized within a specific domain, we next determined the density of gold particles within each bin as a function of PSD area, and of estimated spine or axon terminal volume. A two-way ANOVA demonstrated a main effect of age, but not of treatment, on the density of p-tau gold particles in the presynaptic active zone ($F_{(1,12)} = 12.399$, $p = 0.004$, observed power = 0.898; Fig. 3a, **left**). Tukey’s post hoc tests showed that

active zone p-tau density was significantly lower in axon terminals of aged-V compared to young-V monkeys ($p = 0.024$); the difference between aged-E versus young-V monkeys failed to reach statistical significance ($p = 0.065$). A significant age x treatment interaction was found for p-tau density within the presynaptic cytoplasmic domain (two-way ANOVA; $F_{(1,12)} = 5.32$ $p = 0.04$, observed power = 0.564; Fig. 3a, **middle**). Tukey's posthoc analyses showed that axon terminals of aged-V monkeys had lower cytoplasmic p-tau densities than young monkeys in both treatment groups (aged-V vs. young-V, $p = 2.57 \times 10^{-4}$; aged-V vs. young-E, $p = 0.018$). Axon terminals of aged-E monkeys, however, had a significantly lower cytoplasmic tau density than young-V, but not young-E, monkeys (Tukey's post hoc; aged-E vs. young-V, $p = 0.002$; aged-E vs. young E, $p > 0.05$). A two-way ANOVA demonstrated a main effect of age, but not of treatment, on the density of p-tau gold particles in the plasmalemmal domains ($F_{(1,12)} = 45.665$ $p = 2.00 \times 10^{-5}$, observed power = 1.00; Fig. 3a, **right**). Tukey's posthoc test also revealed that plasmalemmal p-tau density was significantly lower in axon terminals of aged versus young monkeys regardless of estradiol treatment (aged-V vs. young-V, $p = 3.69 \times 10^{-4}$; aged-E vs. young-V, $p = 0.001$; aged-V vs. young-E, $p = 0.003$; aged-E vs. young-E, $p = 0.011$). On the postsynaptic side, a two-way ANOVA showed a significant effect of age on the density of p-tau within the subsynaptic ($F_{(1,12)} = 11.849$, $p = 0.005$, observed power = 0.884), but not any other domain ($p > 0.05$ for all; Fig. 3b). Finally, when the number of p-tau immunogold particles was examined to probe whether changes in synapse size might drive age-dependent reductions in p-tau representation, gold particle numbers were numerically lower in the same 4 presynaptic and postsynaptic domains with age. A trend toward a reduced number of p-tau gold particles in the presynaptic active zone and plasmalemmal domains, and in the postsynaptic subsynaptic domains, was consistent with lower subcellular synaptic representation of ptau in aged compared to young monkeys ($p < 0.08$ for all; data not shown). Taken together, these data indicate that age-dependent decreased pS214-tau immunogold particle density occurs within several presynaptic domains, but postsynaptically, is primarily restricted to the subsynaptic domain.

Relationship between synaptic pS214-tau distributions and DR average accuracy

Abnormally phosphorylated tau is a major component of neurofibrillary tangle pathology in brains of patients with neurodegenerative tauopathies such as Alzheimer's disease where the number of NFTs positively correlates with the degree of synapse and neuron loss, and with the severity of cognitive impairment (Arriagada et al., 1992; Giannakopoulos et al., 2003; Gomez-Isla et al., 1997). Here, bivariate Pearson's correlations were used to evaluate possible relationships between working memory, and synaptic pS214-tau distributions across all monkeys. Synaptic distributions of p-tau showed no correlations with the cognitive status of the monkeys ($p > 0.05$ for all; data not shown).

Relationships between synaptic pS214-tau distributions and synapse density

A substantial literature now supports that several p-tau species are synaptotoxic, and recent studies suggests that pS214-tau may specifically contribute to synaptic vulnerability in aged monkey dlPFC (Carlyle et al., 2014; Crimins, Pooler, Polydoro, Luebke, & Spires-Jones, 2013; Paspalas et al., 2017; Y. Wang & Mandelkow, 2016). Bivariate Pearson's correlations were used to evaluate possible relationships between synapse density, and synaptic p-tau

distributions. Due to the limited number of monkeys and the possible risk for overcorrection, Pearson's correlations were not corrected for multiple comparisons. However, the number of significant correlations detected (6) exceeded that predicted by chance (1). First, a strong positive correlation emerged between synapse density and the sum total number of p-tau immunogold particles separately localized within the axon terminal (Pearson's correlation; $n = 16$ monkeys, $r = 0.525$, $p = 0.037$; data not shown), and dendritic spine (Pearson's correlation; $n = 16$ monkeys, $r = 0.633$, $p = 0.009$; data not shown). When synaptic bins were then examined separately, there was a significant positive correlation between synapse density and the density of p-tau immunogold particles in the cytoplasmic (Pearson's correlation; $n = 16$ monkeys, $r = 0.658$, $p = 0.006$; Fig. 4a, **top**), and plasmalemmal domains (Pearson's correlation; $n = 16$ monkeys, $r = 0.740$, $p = 0.001$; Fig 4a, **bottom**) of axon terminals; and, the subsynaptic (Pearson's correlation; $n = 16$ monkeys, $r = 0.637$, $p = 0.008$; Fig. 4b, **top**), and plasmalemmal (Pearson's correlation; $n = 16$ monkeys, $r = 0.510$, $p = 0.043$; Fig. 4b, **bottom**) domains of dendritic spines.

Discussion

This study revealed a high frequency of synaptic pS214-tau in OVX rhesus monkey dlPFC regardless of age or estradiol treatment. Within the synaptic complex, pS214-tau was predominately enriched in the cytoplasm of axon terminals, and in the synapse and cytoplasm of dendritic spines. Age-dependent loss of synaptic pS214-tau density from presynaptic and postsynaptic domains was associated with synapse loss, but not with cognitive decline. An integrative summary of the proposed relationships between synaptic pS214-tau distributions with aging, and estradiol treatment is schematized in Figure 5.

Age effects on synaptic morphology

Aging was associated with a marked shift toward larger dlPFC synapse spines, as reported previously by our group (Crimins et al., 2017; Dumitriu et al., 2010; Hao et al., 2007). In the present study, we extended this finding to include the presynaptic compartment, and showed a proportional increase in axon terminal diameter. Similar increases in axon terminal size have been previously described in the neostriatum and cortex of aged rodents (Itzev, Lolova, Lolov, & Usunoff, 2001; Mostany et al., 2013). Age-dependent alterations to morphology, such as swelling, could potentially contribute to axon terminal enlargement (Cork et al., 1990; Peters & Sethares, 2002). It is more likely, however, that the presence of relatively fewer small versus large axon terminals, rather than an increase in size affecting the entire population, accounts for this finding. The strong positive correlation between presynaptic and postsynaptic size indices suggests that larger axon terminals form contacts with larger dendritic spines. Such ultrastructural scaling relationships have been previously well documented in the brain, including the cortex (Arellano et al., 2007; Harris & Stevens, 1988, 1989; Lisman & Harris, 1993; Pierce & Lewin, 1994; Yeow & Peterson, 1991). It is worth noting here that since our data were obtained at a single, postmortem time point, it is not possible to establish causal relationships between neurobiological and/or cognitive parameters examined in this study.

Frequency of synapses containing pS214-tau

A high frequency of axon terminals, and of dendritic spines (> 85%) contained pS214tau, which was present in presynaptic and postsynaptic compartments of the same synaptic complex in over three-quarters of synapses, and across age and treatment groups. These findings are in line with those of another recent study wherein ~80% of bipartite neocortical synapses from non-demented elderly control and AD subjects alike were identified as tau-positive (Tai et al., 2014). Like our own observations, modified tau protein (*e.g.* hyperphosphorylated) was also abundantly distributed on both sides of the synapse. The markedly high prevalence of pS214-tau within the monkey dIPFC synaptic complex in the present study indicates that neither advanced age, or the loss of circulating estrogen, is a prerequisite for synaptic pS214-tau immunoreactivity. Its prevalence also suggests that mistrafficking or mislocalization of pS214-tau to the synapse from another neuronal compartment, or its trans-synaptic propagation between neurons—both considered key steps in AD pathogenesis—are not likely part of a disease-related progression of events here (de Calignon et al., 2012; Furman et al., 2017; Hoover et al., 2010; Kfoury, Holmes, Jiang, Holtzman, & Diamond, 2012; L. Liu et al., 2012; Y. Wang & Mandelkow, 2016). Instead, pS214-tau may belong to the molecular profile of normal, healthy monkey dIPFC synapses. Notably, Matsuo et al. (1994) have shown that tau protein from biopsy-derived control human brain is, in fact, phosphorylated at several sites characteristic of advanced neurofibrillary pathology in AD (Matsuo et al., 1994). Normal rodent brain, too, shares several phosphorylated tau epitopes in common with AD brain (Morris et al., 2015). Conversely, similar patterns of tau phosphorylation have been documented in brains from cognitively healthy patients and a mouse model of AD (Matsuo et al., 1994; Morris et al., 2015). AD-like tau phosphorylation has also been reported in other non-disease states, including fetal development, and hibernation (Arendt et al., 2003; Watanabe et al., 1993). Collectively, these observations are compatible with the notion that select p-tau species, like pS214tau, could participate in physiological processes without toxic consequences.

Aside from this one, few studies have aimed to characterize p-tau in brains—let alone synapses—of nonhuman primates, and these have focused nearly exclusively on the paucity of advanced fibrillar pathology in brains of very old subjects (Carlyle et al., 2014; Cramer et al., 2018; Edler et al., 2017; Hartig et al., 2000; Oikawa et al., 2010; Paspalas et al., 2017; Perez et al., 2013; Rosen et al., 2008; Schultz, Hubbard, Rub, Braak, & Braak, 2000). Recently, Carlyle and colleagues (2014) used semi-quantitative single-section post-embedding immuno-EM assessments to show that dendritic spines comprise 4% and 43% of pS214-tau immunoreactive profiles in dIPFC neuropil of young and aged monkeys, respectively; axon terminals were not separately assessed (Carlyle et al., 2014). Since one composite frequency was obtained for each profile type (*i.e.*, the number of immunoreactive axons, dendrites, spines, and non-identified profiles was each expressed as a percentage of the total number of immunoreactive profiles) per age group (versus per monkey, as in the present study), data from this study were largely descriptive, and did not allow for statistical analyses. Consequently, direct comparisons with our own findings are difficult. Such critical differences in immunolabeling analyses, combined with several other methodological discrepancies (*e.g.*, single-section versus serial-section, and pre-embedding versus post-

embedding approaches; and, differences in laminar and synapse-sampling schemes) likely contribute to disparate results between the two studies.

Distributions of synaptic pS214-tau

The present study is the first quantitative investigation of the precise subcellular distributions of pS214-tau immunogold particles across eight defined presynaptic and postsynaptic domains. When frequency data were collapsed across age and treatment groups, we found that pS214-tau was highly enriched in the cytoplasm of both axon terminals and spines. Many cytoplasmic tau immunogold particles were associated with lipid-rich endomembranous structures (*e.g.* the spine apparatus), closely mirroring recent observations by others (Carlyle et al., 2014; Paspalas et al., 2017). In spines, pS214-tau reactivity was also prevalent in the synaptic domain. A smaller proportion (<10%) of pS214-tau immunogold particles was distributed each to presynaptic and postsynaptic plasmalemmas; the presynaptic active zone, and mitochondrial domains; and, to the postsynaptic subsynaptic domain. Such diverse subcellular synaptic distributions support the potential importance of pS214-tau to synaptic integrity in monkey dlPFC.

Our data cannot reveal the precise underlying mechanism by which pS214-tau might play a physiological role within monkey dlPFC synapses, but there are several possibilities. For instance, tau has recently been proposed as a potential mediator of actin and microtubule cytoskeletal network organization; microtubule-dependent transport of critical cargoes such as mitochondria; and, neuronal excitability, including glutamatergic synaptic transmission (Regan, Whitcomb, & Cho, 2016; Y. Wang & Mandelkow, 2016). The latter may partly occur through complex interactions between tau, and the PSD95-GluN2B-Fyn complex (L. M. Ittner et al., 2010; Lau et al., 2016; Mondragon-Rodriguez et al., 2012; Roberson et al., 2011). NMDA receptor activation may, in turn, phosphorylate tau at sites implicated in AD. Direct synaptic stimulation has also since been shown to give rise to phosphorylation of distinct tau residues, and tau phosphorylation may itself be a prerequisite for specific synaptic plasticity events (Frandemiche et al., 2014; Kimura et al., 2014; Kobayashi, Tanaka, Soeda, Almeida, & Takashima, 2017; Regan et al., 2015). Future studies are needed to address the possible relationship between glutamatergic synaptic efficacy and p-tau in monkey dlPFC.

Synaptic pS214-tau and cognitive status

Our data failed to reveal a significant, within-subject association between subcellular distributions of pS214-tau in monkey layer III dlPFC synapses, and individual average performance accuracy on the DR test of working memory. This finding argues against the generalization that p-tau is a clear-cut index of cognitive deterioration. That age-related reductions in pS214-tau immunogold particle density do not appear to be related to cognitive decline in the present study suggest that pS214-tau may be either too far removed from, or does not directly participate in, signaling cascades that linearly influence working memory processes in a close one-to-one association. This finding complements evidence from human studies supporting that accumulation of phosphorylated and/or aggregated tau may not always track cognitive decline, particularly with aging (Bennett, Wilson, Boyle, Buchman, & Schneider, 2012; Boyle, Yu, Wilson, Schneider, & Bennett, 2013; Haroutunian et al.,

2008; Nelson et al., 2010; Rahimi & Kovacs, 2014). However, the absence of association between synaptic pS214tau distributions and working memory performance here does not preclude the possibility that a precise constellation or quantity of tau molecules, exhibiting yet undefined requisite post-translational modification(s), may ultimately be required to influence cognition. The capacity for synaptic tau to trigger cognitive deficits may also be taskdependent, or contingent upon precise cellular and/or regional distributions and actions.

Synaptic pS214-tau levels with age, and their relationship to synapse density

Particularly puzzling was the observation that densities of pS214-tau immunogold particles were significantly lower in aged compared to young monkeys in half of the synaptic domains investigated here. Specifically, an age-dependent loss of pS214-tau density was observed in the presynaptic active zone, cytoplasmic, and plasmalemmal domains; and, the postsynaptic subsynaptic domain. Impaired trafficking of tau to the synapse with aging is one possible explanation for this observation, though this has yet to be tested empirically in our model. Indeed, axonal transport is known to decrease with age, and decreased axonal transport has been invoked as a potential mechanism of neurodegeneration for multiple neurodegenerative disorders, including AD (Ballatore, Lee, & Trojanowski, 2007; Milde, Adalbert, Elaman, & Coleman, 2015; Millecamps & Julien, 2013; Regan et al., 2016). Tau is transported through the axon, and thus, presumably to postsynaptic locations, including spines, as well. Decreased tau transport has been implicated in accumulation of tau in the soma and proximal processes, as a potential early step in NFT formation. However, it also follows that the pool of p-tau that is a natural constituent of the synapse would be affected by decreased transport leading to decreased synaptic tau with age, which is precisely what we observe.

The insensitivity of pS214-tau density to estrogen agrees with OVX rat studies showing stable cortical tau expression, and levels of hyperphosphorylated tau after heat shock, even with hormone replacement regimens (Papazosomenos, 1997; ReynaNeira, Camacho-Arroyo, Ferrera, & Arias, 2002). Though contrary to *in vitro* support for estrogen-dependent attenuation of tau phosphorylation by PKA, that kinases other than PKA alone can phosphorylate tau at the S214 epitope could plausibly account for the lack of treatment effect in the present study (Jicha et al., 1999; F. Liu, Iqbal, GrundkeIqbal, & Gong, 2002; X. A. Liu et al., 2008).

Intriguingly, apart from the presynaptic active zone domain, low pS214-tau densities within each age-sensitive domain, plus the postsynaptic plasmalemmal domain, were significantly associated with lower synapse densities. This was common in aged monkeys regardless of hormone status. On the other hand, young monkeys generally exhibited high pS214-tau densities paired with high synapse densities. The positive relationship between synaptic pS214-tau and spine density further diminishes the likelihood that phosphorylation of tau at the S214 epitope is a synaptotoxic event in monkey dlPFC.

Should a reduction in pS214-tau density signal a loss-of-function event, its absence from the subsynaptic domain may be particularly important to synaptic stability mechanisms. Specifically, tau within the subsynaptic domain is both strategically positioned to directly bind the actin cytoskeleton, and to participate in intracellular signaling cascades critical for

actin remodeling, *e.g.* the MAPK pathway (Cabrales Fontela et al., 2017; Frandemiche et al., 2014; He et al., 2009; Leugers, Koh, Hong, & Lee, 2013; Yamauchi & Purich, 1993). Notably, the interaction between tau and actin leads to accumulation of actin within mouse cortical neuron synapses (Frandemiche et al., 2014). While such cytoskeletal remodeling processes can influence spine stability, it remains to be seen whether tau alters actin structure or stability in monkey dIPFC synapses (Cingolani & Goda, 2008; Matus, 2000). Given that the extended absence of functional glutamatergic receptors can threaten spine stability, disruptions in the targeting and/or anchoring of these receptors may also contribute to spine loss (Cingolani & Goda, 2008; Matus, 2000). It is feasible that pS214-tau participates in glutamate receptor localization to the synapse here, as reported by others, a possibility worth exploring in future work (L. M. Ittner et al., 2010; Lau et al., 2016; Miller et al., 2014; Mondragon-Rodriguez et al., 2012; Suzuki & Kimura, 2017).

High levels of pS214-tau are frequently associated with synapse loss in AD transgenic mouse brain, where human mutant tau is commonly overexpressed severalfold (Crimins et al., 2013). Yet transgenic mouse models, as with nonhuman primates, particularly in the absence of genetic or other experimental manipulations, cannot fully recapitulate all aspects of human AD dementia and brain pathology (Finch & Austad, 2015). While advanced neurofibrillary pathology has been linked to disease severity in AD patients, a recent comprehensive study of human AD Lucifer yellow-injected hippocampal pyramidal neurons showed that synaptic p-tau is not inevitably associated with the loss of dendritic spines (Arriagada et al., 1992; Giannakopoulos et al., 2003; Gomez-Isla et al., 1997; Grundke-Iqbal et al., 1986; Merino-Serrais et al., 2013). Thus, the relationship between p-tau and spine density, even in the context of human neurodegenerative disease, is not always a clear one. That low pS214-tau density accompanied low synapse density here is consistent with reports from recent genesilencing work. For instance, *in vitro* knockdown of tau significantly decreased spine density, and prevented the restoration of hippocampal synapses in response to growth factor stimulation (Chen et al., 2012). Further, disrupted synaptic maintenance was observed in tau deficient aged *Drosophila* neurons (Voelzmann et al., 2016). Tau knockdown was associated with fewer presynaptic specializations during development in this same study. Significant synapse loss has also been observed in aged tau knockout mice (Ma et al., 2014). Collectively, these reports suggest that the loss of a possible synapse-promoting role for tau could contribute to synapse loss.

The robust linear enhancing effect of p-tau on synaptic density opens up the fascinating prospect of its neuroprotective actions on monkey dIPFC synapses. This somewhat unconventional idea is in line with findings from a series of elegant experiments in AD mouse models by Ittner and colleagues (2016) demonstrating inhibition of postsynaptic amyloid- β (A β) excitotoxicity through p38 γ -dependent T205 phosphorylation of tau (A. Ittner et al., 2016). How might phosphorylation of tau at S214 afford synaptic protection? Since the increased propensity of tau toward aggregation has been postulated as important for its trans-synaptic spread, and downstream neurotoxicity, that phosphorylation at the S214 epitope prevents tau fibrillation is one possibility (Eckermann et al., 2007; Furman et al., 2017; Holmes et al., 2014; Kfoury et al., 2012; Schneider, Biernat, von Bergen, Mandelkow, & Mandelkow, 1999). Another option is that early phosphorylation of S214 may prevent neurons from initiating a downstream sequence of pathological phosphorylations required to

generate truly toxic p-tau species (Zheng-Fischhofer et al., 1998). For instance, formation of the epitope for the AT100 antibody highly specific for AD PHF p-tau requires the sequential phosphorylation of Ser/Thr-Pro motifs around the AT8 antibody site (used for Braak staging in AD patients), next of Thr212, and lastly of Ser214. Initial phosphorylation of S214, on the other hand, protects the other sites against phosphorylation, thereby preventing generation of the AT100 epitope (Braak et al., 2006; Braak & Braak, 1995; Zheng-Fischhofer et al., 1998). Protective actions of tau may also be attributed to an as yet unidentified factor interacting at the S214 residue. Any or all of these scenarios might help to explain how pS214-tau could benefit synapses.

Finally, while our data begin to challenge the purely synaptotoxic role for p-tau, one can still imagine several scenarios in which tau is pathogenic here. For instance, if pS214-tau is an early sign of synaptic dysfunction, its presence in young animals could precede the appearance of truly toxic forms with age not examined here. Since tau aggregation and misfolding can occur secondary to abnormal phosphorylation events, it is possible that the pS214 epitope is masked by earlier pathogenic events in aged monkey synapses (Avila, Lucas, Perez, & Hernandez, 2004; Gordon-Krajcer, Yang, & Ksiezak-Reding, 2000). Accumulation of abnormal tau at locations proximal to the synapse could also lead to sequestration of pS214-tau from aged, but not from young, monkey synapses (Alonso, Grundke-Iqbal, Barra, & Iqbal, 1997; Bretteville & Planel, 2008; Congdon & Duff, 2008; Iqbal, Alonso Adel, & Grundke-Iqbal, 2008). From an AD standpoint, A β , though beyond the design of the present study, may be required to “hijack” physiological forms and/or functions of tau, or to act as a pathological “accelerant” to cause synaptic dysfunction (Frandsen et al., 2014; Mondragon-Rodriguez et al., 2012; Pooler et al., 2015). Indeed, a recent study by Jacobs and colleagues (2018) showed a stronger link between aberrant structural connectivity and accumulation of tau pathology in individuals with higher amyloidosis, supporting that A β facilitation of neuronal vulnerability to tau extrapolates to human patients (Jacobs et al., 2018). Our group recently showed that repeated intracerebroventricular injections of soluble oligomers of the A β peptide (A β O) triggers severe spine synapse loss and neuroinflammation, together with increased cerebrospinal fluid levels of A β ₁₋₄₂ and p-tau in dlPFC and hippocampus of female rhesus monkeys. Hence, exogenous A β O administration could be fundamental to establishing a nonhuman primate model of early AD pathogenesis (Beckman et al., 2018).

Conclusions

A comprehensive understanding of molecules pertinent to synaptic health is essential to the development of therapeutic strategies targeting cognitive impairment. Here we quantify pS214-tau distributions across diverse subcellular synaptic domains in rhesus monkey dlPFC with aging and menopause for the first time. We report an agedependent reduction in presynaptic and postsynaptic pS214-tau density that is associated with synapse loss, but not with cognitive status. Together, our results favor a potential physiological role for synaptic pS214-tau in supporting synaptic stability, and highlight the possibility that AD-like proteopathic processes in rhesus macaques may distinctly differ from those known to occur in AD patients.

Acknowledgements

We thank Mary Roberts, Sania Fong, Deborah Kent, Heather McKay, Tweithy Oung, and Anne Canfield at the California National Primate Research Center for technical assistance with rhesus monkeys, and Dr. Donald Canfield for veterinary work. We also thank Dr. Peter Davies at The Feinstein Institute for Medical Research for the generous gift of the anti-pS214-tau (CP3) antibody. This work was supported by National Institute on Aging grant P01 AG16765 to J.H.M., and in part by the Intramural Research Program of the National Institute on Aging.

References

- Allen B, Ingram E, Takao M, Smith MJ, Jakes R, Virdee K, ... Goedert M (2002). Abundant tau filaments and nonapoptotic neurodegeneration in transgenic mice expressing human P301S tau protein. *J Neurosci*, 22(21), 9340–9351. [PubMed: 12417659]
- Alonso AD, Grundke-Iqbal I, Barra HS, & Iqbal K (1997). Abnormal phosphorylation of tau and the mechanism of Alzheimer neurofibrillary degeneration: sequestration of microtubule-associated proteins 1 and 2 and the disassembly of microtubules by the abnormal tau. *Proc Natl Acad Sci U S A*, 94(1), 298–303. [PubMed: 8990203]
- Alvarez-de-la-Rosa M, Silva I, Nilsen J, Perez MM, Garcia-Segura LM, Avila J, & Naftolin F (2005). Estradiol prevents neural tau hyperphosphorylation characteristic of Alzheimer's disease. *Ann N Y Acad Sci*, 1052, 210–224. 10.1196/annals.1347.016 [PubMed: 16024764]
- Andersen K, Launer LJ, Dewey ME, Letenneur L, Ott A, Copeland JR, ... Hofman A (1999). Gender differences in the incidence of AD and vascular dementia: The EURODEM Studies. EURODEM Incidence Research Group. *Neurology*, 53(9), 1992–1997. [PubMed: 10599770]
- Arellano JI, Benavides-Piccione R, Defelipe J, & Yuste R (2007). Ultrastructure of dendritic spines: correlation between synaptic and spine morphologies. *Front Neurosci*, 1(1), 131–143. 10.3389/neuro.01.1.1.010.2007 [PubMed: 18982124]
- Arendt T, Stieler J, Strijkstra AM, Hut RA, Rudiger J, Van der Zee EA, ... Hartig W (2003). Reversible paired helical filament-like phosphorylation of tau is an adaptive process associated with neuronal plasticity in hibernating animals. *J Neurosci*, 23(18), 6972–6981. [PubMed: 12904458]
- Arnsten AF, Wang MJ, & Paspalas CD (2012). Neuromodulation of thought: flexibilities and vulnerabilities in prefrontal cortical network synapses. *Neuron*, 76(1), 223–239. 10.1016/j.neuron.2012.08.038 [PubMed: 23040817]
- Arriagada PV, Growdon JH, Hedley-Whyte ET, & Hyman BT (1992). Neurofibrillary tangles but not senile plaques parallel duration and severity of Alzheimer's disease. *Neurology*, 42(3 Pt 1), 631–639. [PubMed: 1549228]
- Augustinack JC, Schneider A, Mandelkow EM, & Hyman BT (2002). Specific tau phosphorylation sites correlate with severity of neuronal cytopathology in Alzheimer's disease. *Acta Neuropathol*, 103(1), 26–35. [PubMed: 11837744]
- Avila J, Lucas JJ, Perez M, & Hernandez F (2004). Role of tau protein in both physiological and pathological conditions. *Physiol Rev*, 84(2), 361–384. 10.1152/physrev.00024.2003 [PubMed: 15044677]
- Ballatore C, Lee VM, & Trojanowski JQ (2007). Tau-mediated neurodegeneration in Alzheimer's disease and related disorders. *Nat Rev Neurosci*, 8(9), 663–672. 10.1038/nrn2194 [PubMed: 17684513]
- Bartus RT, Fleming D, & Johnson HR (1978). Aging in the rhesus monkey: debilitating effects on short-term memory. *J Gerontol*, 33(6), 858–871. [PubMed: 106081]
- Beckman D, Donis-Cox K, Ott S, Roberts M, Novik L, Janssen WG, ... Morrison JH (2018). Quantitative analysis of synaptic pathology and neuroinflammation: an initial study in a female rhesus monkey model of the "synaptic" phase of Alzheimer's disease. *bioRxiv*(doi: 10.1101/251025).
- Bennett DA, Wilson RS, Boyle PA, Buchman AS, & Schneider JA (2012). Relation of neuropathology to cognition in persons without cognitive impairment. *Ann Neurol*, 72(4), 599–609. 10.1002/ana.23654 [PubMed: 23109154]

- Black MM, Slaughter T, Moshiaich S, Obrocka M, & Fischer I (1996). Tau is enriched on dynamic microtubules in the distal region of growing axons. *J Neurosci*, 16(11), 3601–3619. [PubMed: 8642405]
- Bove R, Secor E, Chibnik LB, Barnes LL, Schneider JA, Bennett DA, & De Jager PL (2014). Age at surgical menopause influences cognitive decline and Alzheimer pathology in older women. *Neurology*, 82(3), 222–229. 10.1212/WNL.000000000000033 [PubMed: 24336141]
- Boyle PA, Yu L, Wilson RS, Schneider JA, & Bennett DA (2013). Relation of neuropathology with cognitive decline among older persons without dementia. *Front Aging Neurosci*, 5, 50. 10.3389/fnagi.2013.00050 [PubMed: 24058343]
- Braak H, Alafuzoff I, Arzberger T, Kretschmar H, & Del Tredici K (2006). Staging of Alzheimer disease-associated neurofibrillary pathology using paraffin sections and immunocytochemistry. *Acta Neuropathol*, 112(4), 389–404. 10.1007/s00401-006-0127-z [PubMed: 16906426]
- Braak H, & Braak E (1995). Staging of Alzheimer's disease-related neurofibrillary changes. *Neurobiol Aging*, 16(3), 271–278; discussion 278–284. [PubMed: 7566337]
- Braak H, Thal DR, Ghebremedhin E, & Del Tredici K (2011). Stages of the pathologic process in Alzheimer disease: age categories from 1 to 100 years. *J Neuropathol Exp Neurol*, 70(11), 960–969. 10.1097/NEN.0b013e318232a379 [PubMed: 22002422]
- Bretteville A, & Planel E (2008). Tau aggregates: toxic, inert, or protective species? *J Alzheimers Dis*, 14(4), 431–436. [PubMed: 18688094]
- Brinton RD (2009). Estrogen-induced plasticity from cells to circuits: predictions for cognitive function. *Trends Pharmacol Sci*, 30(4), 212–222. 10.1016/j.tips.2008.12.006 [PubMed: 19299024]
- Brookmeyer R, Johnson E, Ziegler-Graham K, & Arrighi HM (2007). Forecasting the global burden of Alzheimer's disease. *Alzheimers Dement*, 3(3), 186–191. 10.1016/j.jalz.2007.04.381 [PubMed: 19595937]
- Cabrales Fontela Y, Kadavath H, Biernat J, Riedel D, Mandelkow E, & Zweckstetter M (2017). Multivalent cross-linking of actin filaments and microtubules through the microtubule-associated protein Tau. *Nat Commun*, 8(1), 1981. 10.1038/s41467-017-02230-8 [PubMed: 29215007]
- Carlyle BC, Nairn AC, Wang M, Yang Y, Jin LE, Simen AA, ... Paspalas CD (2014). cAMP-PKA phosphorylation of tau confers risk for degeneration in aging association cortex. *Proc Natl Acad Sci U S A*, 111(13), 5036–5041. 10.1073/pnas.1322360111 [PubMed: 24707050]
- Chen Q, Zhou Z, Zhang L, Wang Y, Zhang YW, Zhong M, ... Yu ZP (2012). Tau protein is involved in morphological plasticity in hippocampal neurons in response to BDNF. *Neurochem Int*, 60(3), 233–242. 10.1016/j.neuint.2011.12.013 [PubMed: 22226842]
- Cingolani LA, & Goda Y (2008). Actin in action: the interplay between the actin cytoskeleton and synaptic efficacy. *Nat Rev Neurosci*, 9(5), 344–356. 10.1038/nrn2373 [PubMed: 18425089]
- Colonnier M, & Beaulieu C (1985). An empirical assessment of stereological formulae applied to the counting of synaptic disks in the cerebral cortex. *J Comp Neurol*, 231(2), 175–179. 10.1002/cne.902310205 [PubMed: 3881485]
- Congdon EE, & Duff KE (2008). Is tau aggregation toxic or protective? *J Alzheimers Dis*, 14(4), 453–457. [PubMed: 18688098]
- Cork LC, Masters C, Beyreuther K, & Price DL (1990). Development of senile plaques. Relationships of neuronal abnormalities and amyloid deposits. *Am J Pathol*, 137(6), 1383–1392. [PubMed: 1701963]
- Cramer PE, Gentzel RC, Tanis KQ, Vardigan J, Wang Y, Connolly B, ... Uslander JM (2018). Aging African green monkeys manifest transcriptional, pathological, and cognitive hallmarks of human Alzheimer's disease. *Neurobiol Aging*, 64, 92–106. 10.1016/j.neurobiolaging.2017.12.011 [PubMed: 29353102]
- Crimins JL, Pooler A, Polydoro M, Luebke JI, & Spires-Jones TL (2013). The intersection of amyloid beta and tau in glutamatergic synaptic dysfunction and collapse in Alzheimer's disease. *Ageing Res Rev*, 12(3), 757–763. 10.1016/j.arr.2013.03.002 [PubMed: 23528367]
- Crimins JL, Wang AC, Yuk F, Puri R, Janssen WGM, Hara Y, ... Morrison JH (2017). Diverse Synaptic Distributions of G Protein-coupled Estrogen Receptor 1 in Monkey Prefrontal Cortex with Aging and Menopause. *Cereb Cortex*, 27(3), 2022–2033. 10.1093/cercor/bhw050 [PubMed: 26941383]

- de Calignon A, Polydoro M, Suarez-Calvet M, William C, Adamowicz DH, Kopeikina KJ, ... Hyman BT (2012). Propagation of tau pathology in a model of early Alzheimer's disease. *Neuron*, 73(4), 685–697. [10.1016/j.neuron.2011.11.033](https://doi.org/10.1016/j.neuron.2011.11.033) [PubMed: 22365544]
- Dumitriu D, Hao J, Hara Y, Kaufmann J, Janssen WG, Lou W, ... Morrison JH (2010). Selective changes in thin spine density and morphology in monkey prefrontal cortex correlate with aging-related cognitive impairment. *J Neurosci*, 30(22), 7507–7515. [10.1523/JNEUROSCI.6410-09.2010](https://doi.org/10.1523/JNEUROSCI.6410-09.2010) [PubMed: 20519525]
- Eckermann K, Mocanu MM, Khlistunova I, Biernat J, Nissen A, Hofmann A, ... Mandelkow EM (2007). The beta-propensity of Tau determines aggregation and synaptic loss in inducible mouse models of tauopathy. *J Biol Chem*, 282(43), 31755–31765. [10.1074/jbc.M705282200](https://doi.org/10.1074/jbc.M705282200) [PubMed: 17716969]
- Eidler MK, Sherwood CC, Meindl RS, Hopkins WD, Ely JJ, Erwin JM, ... Raghanti MA (2017). Aged chimpanzees exhibit pathologic hallmarks of Alzheimer's disease. *Neurobiol Aging*, 59, 107–120. [10.1016/j.neurobiolaging.2017.07.006](https://doi.org/10.1016/j.neurobiolaging.2017.07.006) [PubMed: 28888720]
- Finch CE, & Austad SN (2015). Commentary: is Alzheimer's disease uniquely human? *Neurobiol Aging*, 36(2), 553–555. [10.1016/j.neurobiolaging.2014.10.025](https://doi.org/10.1016/j.neurobiolaging.2014.10.025) [PubMed: 25533426]
- Frandemiche ML, De Seranno S, Rush T, Borel E, Elie A, Arnal I, ... Buisson A (2014). Activity-dependent tau protein translocation to excitatory synapse is disrupted by exposure to amyloid-beta oligomers. *J Neurosci*, 34(17), 6084–6097. [10.1523/JNEUROSCI.4261-13.2014](https://doi.org/10.1523/JNEUROSCI.4261-13.2014) [PubMed: 24760868]
- Funahashi S, Bruce CJ, & Goldman-Rakic PS (1989). Mnemonic coding of visual space in the monkey's dorsolateral prefrontal cortex. *J Neurophysiol*, 61(2), 331–349. [PubMed: 2918358]
- Furman JL, Vaquer-Alicea J, White CL, 3rd, Cairns NJ, Nelson PT, & Diamond MI (2017). Widespread tau seeding activity at early Braak stages. *Acta Neuropathol*, 133(1), 91–100. [10.1007/s00401-016-1644-z](https://doi.org/10.1007/s00401-016-1644-z) [PubMed: 27878366]
- Gearing M, Tigges J, Mori H, & Mirra SS (1996). A beta40 is a major form of betaamyloid in nonhuman primates. *Neurobiol Aging*, 17(6), 903–908. [PubMed: 9363802]
- Giannakopoulos P, Herrmann FR, Bussiere T, Bouras C, Kovari E, Perl DP ... Hof PR (2003). Tangle and neuron numbers, but not amyloid load, predict cognitive status in Alzheimer's disease. *Neurology*, 60(9), 1495–1500. [PubMed: 12743238]
- Gilardi KV, Shideler SE, Valverde CR, Roberts JA, & Lasley BL (1997). Characterization of the onset of menopause in the rhesus macaque. *Biol Reprod*, 57(2), 335–340. [PubMed: 9241047]
- Gill S, Sharpless JL, Rado K, & Hall JE (2002). Evidence that GnRH decreases with gonadal steroid feedback but increases with age in postmenopausal women. *J Clin Endocrinol Metab*, 87(5), 2290–2296. [10.1210/jcem.87.5.8508](https://doi.org/10.1210/jcem.87.5.8508) [PubMed: 11994378]
- Gleason CE, Dowling NM, Wharton W, Manson JE, Miller VM, Atwood CS, ... Asthana S (2015). Effects of Hormone Therapy on Cognition and Mood in Recently Postmenopausal Women: Findings from the Randomized, Controlled KEEPS-Cognitive and Affective Study. *PLoS Med*, 12(6), e1001833; discussion e1001833. [10.1371/journal.pmed.1001833](https://doi.org/10.1371/journal.pmed.1001833) [PubMed: 26035291]
- Goldman-Rakic PS (1995). Cellular basis of working memory. *Neuron*, 14(3), 477–485. [PubMed: 7695894]
- Gomez-Isla T, Hollister R, West H, Mui S, Growdon JH, Petersen RC, ... Hyman BT (1997). Neuronal loss correlates with but exceeds neurofibrillary tangles in Alzheimer's disease. *Ann Neurol*, 41(1), 17–24. [10.1002/ana.410410106](https://doi.org/10.1002/ana.410410106) [PubMed: 9005861]
- Goodenough S, Schleusner D, Pietrzik C, Skutella T, & Behl C (2005). Glycogen synthase kinase 3beta links neuroprotection by 17beta-estradiol to key Alzheimer processes. *Neuroscience*, 132(3), 581–589. [10.1016/j.neuroscience.2004.12.029](https://doi.org/10.1016/j.neuroscience.2004.12.029) [PubMed: 15837120]
- Gordon-Krajcer W, Yang L, & Ksiezak-Reding H (2000). Conformation of paired helical filaments blocks dephosphorylation of epitopes shared with fetal tau except Ser199/202 and Ser202/Thr205. *Brain Res*, 856(1–2), 163–175. [PubMed: 10677623]
- Grundke-Iqbal I, Iqbal K, Quinlan M, Tung YC, Zaidi MS, & Wisniewski HM (1986). Microtubule-associated protein tau. A component of Alzheimer paired helical filaments. *J Biol Chem*, 261(13), 6084–6089. [PubMed: 3084478]

- Hao J, Rapp PR, Janssen WG, Lou W, Lasley BL, Hof PR, & Morrison JH (2007). Interactive effects of age and estrogen on cognition and pyramidal neurons in monkey prefrontal cortex. *Proc Natl Acad Sci U S A*, 104(27), 11465–11470. 10.1073/pnas.0704757104 [PubMed: 17592140]
- Hao J, Rapp PR, Leffler AE, Leffler SR, Janssen WG, Lou W, ... Morrison JH (2006). Estrogen alters spine number and morphology in prefrontal cortex of aged female rhesus monkeys. *J Neurosci*, 26(9), 2571–2578. 10.1523/JNEUROSCI.3440-05.2006 [PubMed: 16510735]
- Hara Y, Punsoni M, Yuk F, Park CS, Janssen WG, Rapp PR, & Morrison JH (2012). Synaptic distributions of GluA2 and PKMzeta in the monkey dentate gyrus and their relationships with aging and memory. *J Neurosci*, 32(21), 7336–7344. 10.1523/JNEUROSCI.0605-12.2012 [PubMed: 22623679]
- Hara Y, Rapp PR, & Morrison JH (2012). Neuronal and morphological bases of cognitive decline in aged rhesus monkeys. *Age (Dordr)*, 34(5), 1051–1073. 10.1007/s11357-011-9278-5 [PubMed: 21710198]
- Hara Y, Waters EM, McEwen BS, & Morrison JH (2015). Estrogen Effects on Cognitive and Synaptic Health Over the Lifecourse. *Physiol Rev*, 95(3), 785–807. 10.1152/physrev.00036.2014 [PubMed: 26109339]
- Hara Y, Yuk F, Puri R, Janssen WG, Rapp PR, & Morrison JH (2014). Presynaptic mitochondrial morphology in monkey prefrontal cortex correlates with working memory and is improved with estrogen treatment. *Proc Natl Acad Sci U S A*, 111(1), 486–491. 10.1073/pnas.1311310110 [PubMed: 24297907]
- Hara Y, Yuk F, Puri R, Janssen WG, Rapp PR, & Morrison JH (2016). Estrogen Restores Multisynaptic Boutons in the Dorsolateral Prefrontal Cortex while Promoting Working Memory in Aged Rhesus Monkeys. *J Neurosci*, 36(3), 901–910. 10.1523/JNEUROSCI.3480-13.2016 [PubMed: 26791219]
- Haroutunian V, Schnaider-Beeri M, Schmeidler J, Wysocki M, Purohit DP, Perl DP, ... Grossman HT (2008). Role of the neuropathology of Alzheimer disease in dementia in the oldest-old. *Arch Neurol*, 65(9), 1211–1217. 10.1001/archneur.65.9.1211 [PubMed: 18779425]
- Harris KM, & Stevens JK (1988). Dendritic spines of rat cerebellar Purkinje cells: serial electron microscopy with reference to their biophysical characteristics. *J Neurosci*, 8(12), 4455–4469. [PubMed: 3199186]
- Harris KM, & Stevens JK (1989). Dendritic spines of CA 1 pyramidal cells in the rat hippocampus: serial electron microscopy with reference to their biophysical characteristics. *J Neurosci*, 9(8), 2982–2997. [PubMed: 2769375]
- Hartig W, Klein C, Brauer K, Schuppel KF, Arendt T, Bruckner G, & Bigl V (2000). Abnormally phosphorylated protein tau in the cortex of aged individuals of various mammalian orders. *Acta Neuropathol*, 100(3), 305–312. [PubMed: 10965801]
- He HJ, Wang XS, Pan R, Wang DL, Liu MN, & He RQ (2009). The proline-rich domain of tau plays a role in interactions with actin. *BMC Cell Biol*, 10, 81. 10.1186/1471-2121-10-81 [PubMed: 19895707]
- Henderson VW, Benke KS, Green RC, Cupples LA, Farrer LA, & Group MS (2005). Postmenopausal hormone therapy and Alzheimer's disease risk: interaction with age. *J Neurol Neurosurg Psychiatry*, 76(1), 103–105. 10.1136/jnnp.2003.024927 [PubMed: 15608005]
- Holmes BB, Furman JL, Mahan TE, Yamasaki TR, Mirbaha H, Eades WC, ... Diamond MI (2014). Proteopathic tau seeding predicts tauopathy in vivo. *Proc Natl Acad Sci U S A*, 111(41), E4376–4385. 10.1073/pnas.1411649111 [PubMed: 25261551]
- Hoover BR, Reed MN, Su J, Penrod RD, Kotilinek LA, Grant MK, ... Liao D (2010). Tau mislocalization to dendritic spines mediates synaptic dysfunction independently of neurodegeneration. *Neuron*, 68(6), 1067–1081. 10.1016/j.neuron.2010.11.030 [PubMed: 21172610]
- Hung SY, & Fu WM (2017). Drug candidates in clinical trials for Alzheimer's disease. *J Biomed Sci*, 24(1), 47. 10.1186/s12929-017-0355-7 [PubMed: 28720101]
- Iqbal K, Alonso Adel C, & Grundke-Iqbal I (2008). Cytosolic abnormally hyperphosphorylated tau but not paired helical filaments sequester normal MAPs and inhibit microtubule assembly. *J Alzheimers Dis*, 14(4), 365–370. [PubMed: 18688085]

- Ittner A, Chua SW, Bertz J, Volkerling A, van der Hoven J, Gladbach A, ... Ittner LM (2016). Site-specific phosphorylation of tau inhibits amyloid-beta toxicity in Alzheimer's mice. *Science*, 354(6314), 904–908. 10.1126/science.aah6205 [PubMed: 27856911]
- Ittner LM, Ke YD, Delerue F, Bi M, Gladbach A, van Eersel J, ... Gotz J (2010). Dendritic function of tau mediates amyloid-beta toxicity in Alzheimer's disease mouse models. *Cell*, 142(3), 387–397. 10.1016/j.cell.2010.06.036 [PubMed: 20655099]
- Itzev D, Lolova I, Lolov S, & Usunoff KG (2001). Age-related changes in the synapses of the rat's neostriatum. *Arch Physiol Biochem*, 109(1), 80–89. 10.1076/apab.109.1.80.4279 [PubMed: 11471075]
- Jacobs HIL, Hedden T, Schultz AP, Sepulcre J, Perea RD, Amariglio RE, ... Johnson KA (2018). Structural tract alterations predict downstream tau accumulation in amyloid-positive older individuals. *Nat Neurosci*, 21(3), 424–431. 10.1038/s41593-018-0070-z [PubMed: 29403032]
- Jicha GA, Weaver C, Lane E, Vianna C, Kress Y, Rockwood J, & Davies P (1999). cAMP-dependent protein kinase phosphorylations on tau in Alzheimer's disease. *J Neurosci*, 19(17), 7486–7494. [PubMed: 10460255]
- Kantarci K, Lowe VJ, Lesnick TG, Tosakulwong N, Bailey KR, Fields JA, ... Miller VM (2016). Early Postmenopausal Transdermal 17beta-Estradiol Therapy and Amyloid-beta Deposition. *J Alzheimers Dis*, 53(2), 547–556. 10.3233/JAD-160258 [PubMed: 27163830]
- Kantarci K, Tosakulwong N, Lesnick TG, Zuk SM, Lowe VJ, Fields JA, ... Miller VM (2018). Brain structure and cognition 3 years after the end of an early menopausal hormone therapy trial. *Neurology*, 0(e1–e9).
- Kempf M, Clement A, Faissner A, Lee G, & Brandt R (1996). Tau binds to the distal axon early in development of polarity in a microtubule- and microfilamentdependent manner. *J Neurosci*, 16(18), 5583–5592. [PubMed: 8795614]
- Kfoury N, Holmes BB, Jiang H, Holtzman DM, & Diamond MI (2012). Transcellular propagation of Tau aggregation by fibrillar species. *J Biol Chem*, 287(23), 19440–19451. 10.1074/jbc.M112.346072 [PubMed: 22461630]
- Kimura T, Whitcomb DJ, Jo J, Regan P, Piers T, Heo S, ... Cho K (2014). Microtubule-associated protein tau is essential for long-term depression in the hippocampus. *Philos Trans R Soc Lond B Biol Sci*, 369(1633), 20130144 10.1098/rstb.2013.0144 [PubMed: 24298146]
- Kobayashi S, Tanaka T, Soeda Y, Almeida OFX, & Takashima A (2017). Local Somatodendritic Translation and Hyperphosphorylation of Tau Protein Triggered by AMPA and NMDA Receptor Stimulation. *EBioMedicine*, 20, 120–126. 10.1016/j.ebiom.2017.05.012 [PubMed: 28566250]
- Lacreuse A, Mong JA, & Hara Y (2015). Neurocognitive effects of estrogens across the adult lifespan in nonhuman primates: State of knowledge and new perspectives. *Horm Behav*, 74, 157–166. 10.1016/j.yhbeh.2015.03.001 [PubMed: 25762288]
- Lau DH, Hogseth M, Phillips EC, O'Neill MJ, Pooler AM, Noble W, & Hanger DP (2016). Critical residues involved in tau binding to fyn: implications for tau phosphorylation in Alzheimer's disease. *Acta Neuropathol Commun*, 4(1), 49 10.1186/s40478-016-0317-4 [PubMed: 27193083]
- Laws KR, Irvine K, & Gale TM (2016). Sex differences in cognitive impairment in Alzheimer's disease. *World J Psychiatry*, 6(1), 54–65. 10.5498/wjp.v6.i1.54 [PubMed: 27014598]
- Leugers CJ, Koh JY, Hong W, & Lee G (2013). Tau in MAPK activation. *Front Neurol*, 4, 161 10.3389/fneur.2013.00161 [PubMed: 24146661]
- Lewis J, Dickson DW, Lin WL, Chisholm L, Corral A, Jones G, ... McGowan E (2001). Enhanced neurofibrillary degeneration in transgenic mice expressing mutant tau and APP. *Science*, 293(5534), 1487–1491. 10.1126/science.1058189 [PubMed: 11520987]
- Lewis J, McGowan E, Rockwood J, Melrose H, Nacharaju P, Van Slegtenhorst M, ... Hutton M (2000). Neurofibrillary tangles, amyotrophy and progressive motor disturbance in mice expressing mutant (P301L) tau protein. *Nat Genet*, 25(4), 402–405. 10.1038/78078 [PubMed: 10932182]
- Lisman JE, & Harris KM (1993). Quantal analysis and synaptic anatomy-integrating two views of hippocampal plasticity. *Trends Neurosci*, 16(4), 141–147. [PubMed: 7682347]
- Liu F, Iqbal K, Grundke-Iqbal I, & Gong CX (2002). Involvement of aberrant glycosylation in phosphorylation of tau by cdk5 and GSK-3beta. *FEBS Lett*, 530(1–3), 209–214. [PubMed: 12387894]

- Liu L, Drouet V, Wu JW, Witter MP, Small SA, Clelland C, & Duff K (2012). Trans-synaptic spread of tau pathology in vivo. *PLoS One*, 7(2), e31302 10.1371/journal.pone.0031302 [PubMed: 22312444]
- Liu XA, Zhu LQ, Zhang Q, Shi HR, Wang SH, Wang Q, & Wang JZ (2008). Estradiol attenuates tau hyperphosphorylation induced by upregulation of protein kinase-A. *Neurochem Res*, 33(9), 1811–1820. 10.1007/s11064-008-9638-4 [PubMed: 18338250]
- Loerch PM, Lu T, Dakin KA, Vann JM, Isaacs A, Geula C, ... Yankner BA (2008). Evolution of the aging brain transcriptome and synaptic regulation. *PLoS One*, 3(10), e3329 10.1371/journal.pone.0003329 [PubMed: 18830410]
- Ma QL, Zuo X, Yang F, Ubeda OJ, Gant DJ, Alaverdyan M, ... Cole GM (2014). Loss of MAP function leads to hippocampal synapse loss and deficits in the Morris Water Maze with aging. *J Neurosci*, 34(21), 7124–7136. 10.1523/JNEUROSCI.3439-13.2014 [PubMed: 24849348]
- Matsuo ES, Shin RW, Billingsley ML, Van de Voorde A, O'Connor M, Trojanowski JQ, & Lee VM (1994). Biopsy-derived adult human brain tau is phosphorylated at many of the same sites as Alzheimer's disease paired helical filament tau. *Neuron*, 13(4), 989–1002. [PubMed: 7946342]
- Matt DW, Kauma SW, Pincus SM, Veldhuis JD, & Evans WS (1998). Characteristics of luteinizing hormone secretion in younger versus older premenopausal women. *Am J Obstet Gynecol*, 178(3), 504–510. [PubMed: 9539517]
- Matus A (2000). Actin-based plasticity in dendritic spines. *Science*, 290(5492), 754–758. [PubMed: 11052932]
- Merino-Serrais P, Benavides-Piccione R, Blazquez-Llorca L, Kastanauskaite A, Rabano A, Avila J, & DeFelipe J (2013). The influence of phospho-tau on dendritic spines of cortical pyramidal neurons in patients with Alzheimer's disease. *Brain*, 136(Pt 6), 1913–1928. 10.1093/brain/awt088 [PubMed: 23715095]
- Merlo S, Spampinato SF, & Sortino MA (2017). Estrogen and Alzheimer's disease: Still an attractive topic despite disappointment from early clinical results. *Eur J Pharmacol*, 817, 51–58. 10.1016/j.ejphar.2017.05.059 [PubMed: 28577965]
- Milde S, Adalbert R, Elaman MH, & Coleman MP (2015). Axonal transport declines with age in two distinct phases separated by a period of relative stability. *Neurobiol Aging*, 36(2), 971–981. 10.1016/j.neurobiolaging.2014.09.018 [PubMed: 25443288]
- Millecamps S, & Julien JP (2013). Axonal transport deficits and neurodegenerative diseases. *Nat Rev Neurosci*, 14(3), 161–176. 10.1038/nrn3380 [PubMed: 23361386]
- Miller EC, Teravskis PJ, Dummer BW, Zhao X, Huganir RL, & Liao D (2014). Tau phosphorylation and tau mislocalization mediate soluble Aβ oligomer-induced AMPA glutamate receptor signaling deficits. *Eur J Neurosci*, 39(7), 1214–1224. 10.1111/ejn.12507 [PubMed: 24713000]
- Mondragon-Rodriguez S, Trillaud-Doppia E, Dudilot A, Bourgeois C, Lauzon M, Leclerc N, & Boehm J (2012). Interaction of endogenous tau protein with synaptic proteins is regulated by N-methyl-D-aspartate receptor-dependent tau phosphorylation. *J Biol Chem*, 287(38), 32040–32053. 10.1074/jbc.M112.401240 [PubMed: 22833681]
- Morris M, Knudsen GM, Maeda S, Trinidad JC, Ioanoviciu A, Burlingame AL, & Mucke L (2015). Tau post-translational modifications in wild-type and human amyloid precursor protein transgenic mice. *Nat Neurosci*, 18(8), 1183–1189. 10.1038/nn.4067 [PubMed: 26192747]
- Morrison JH, & Baxter MG (2012). The ageing cortical synapse: hallmarks and implications for cognitive decline. *Nat Rev Neurosci*, 13(4), 240–250. 10.1038/nrn3200 [PubMed: 22395804]
- Morrison JH, & Hof PR (2002). Selective vulnerability of corticocortical and hippocampal circuits in aging and Alzheimer's disease. *Prog Brain Res*, 136, 467–486. [PubMed: 12143403]
- Mostany R, Anstey JE, Crump KL, Maco B, Knott G, & Portera-Cailliau C (2013). Altered synaptic dynamics during normal brain aging. *J Neurosci*, 33(9), 4094–4104. 10.1523/JNEUROSCI.4825-12.2013 [PubMed: 23447617]
- Nagahara AH, Bernot T, & Tuszyński MH (2010). Age-related cognitive deficits in rhesus monkeys mirror human deficits on an automated test battery. *Neurobiol Aging*, 31(6), 1020–1031. 10.1016/j.neurobiolaging.2008.07.007 [PubMed: 18760505]
- Nelson PT, Abner EL, Schmitt FA, Kryscio RJ, Jicha GA, Smith CD, ... Markesbery WR (2010). Modeling the association between 43 different clinical and pathological variables and the severity

- of cognitive impairment in a large autopsy cohort of elderly persons. *Brain Pathol*, 20(1), 66–79. 10.1111/j.1750-3639.2008.00244.x [PubMed: 19021630]
- Nelson PT, Alafuzoff I, Bigio EH, Bouras C, Braak H, Cairns NJ, ... Beach TG (2012). Correlation of Alzheimer disease neuropathologic changes with cognitive status: a review of the literature. *J Neuropathol Exp Neurol*, 71(5), 362–381. 10.1097/NEN.0b013e31825018f7 [PubMed: 22487856]
- Nichols SM, Bavister BD, Brenner CA, Didier PJ, Harrison RM, & Kubisch HM (2005). Ovarian senescence in the rhesus monkey (*Macaca mulatta*). *Hum Reprod*, 20(1), 79–83. 10.1093/humrep/deh576 [PubMed: 15498779]
- Oikawa N, Kimura N, & Yanagisawa K (2010). Alzheimer-type tau pathology in advanced aged nonhuman primate brains harboring substantial amyloid deposition. *Brain Res*, 1315, 137–149. 10.1016/j.brainres.2009.12.005 [PubMed: 20004650]
- Papasozomenos SC (1997). The heat shock-induced hyperphosphorylation of tau is estrogen-independent and prevented by androgens: implications for Alzheimer disease. *Proc Natl Acad Sci U S A*, 94(13), 6612–6617. [PubMed: 9192613]
- Paspalas CD, Carlyle BC, Leslie S, Preuss TM, Crimins JL, Huttner AJ, ... Arnsten AFT (2017). The aged rhesus macaque manifests Braak stage III/IV Alzheimer's-like pathology. *Alzheimers Dement* 10.1016/j.jalz.2017.11.005
- Perez SE, Raghanti MA, Hof PR, Kramer L, Ikonovic MD, Lacor PN, ... Mufson EJ (2013). Alzheimer's disease pathology in the neocortex and hippocampus of the western lowland gorilla (*Gorilla gorilla gorilla*). *J Comp Neurol*, 521(18), 4318–4338. 10.1002/cne.23428 [PubMed: 23881733]
- Peters A, & Morrison JH (1999). *Cerebral cortex: neurodegenerative and age-related changes in structure and function of cerebral cortex* New York: Springer.
- Peters A, & Sethares C (2002). Aging and the myelinated fibers in prefrontal cortex and corpus callosum of the monkey. *J Comp Neurol*, 442(3), 277–291. [PubMed: 11774342]
- Peters A, Sethares C, & Luebke JI (2008). Synapses are lost during aging in the primate prefrontal cortex. *Neuroscience*, 152(4), 970–981. 10.1016/j.neuroscience.2007.07.014 [PubMed: 18329176]
- Petrides M, & Pandya DN (1999). Dorsolateral prefrontal cortex: comparative cytoarchitectonic analysis in the human and the macaque brain and corticocortical connection patterns. *Eur J Neurosci*, 11(3), 1011–1036. [PubMed: 10103094]
- Phung TK, Waltoft BL, Laursen TM, Settnes A, Kessing LV, Mortensen PB, & Waldemar G (2010). Hysterectomy, oophorectomy and risk of dementia: a nationwide historical cohort study. *Dement Geriatr Cogn Disord*, 30(1), 43–50. 10.1159/000314681 [PubMed: 20689282]
- Pierce JP, & Lewin GR (1994). An ultrastructural size principle. *Neuroscience*, 58(3), 441–446. [PubMed: 8170532]
- Pike CJ (2017). Sex and the development of Alzheimer's disease. *J Neurosci Res*, 95(1–2), 671–680. 10.1002/jnr.23827 [PubMed: 27870425]
- Pooler AM, Polydoro M, Maury EA, Nicholls SB, Reddy SM, Wegmann S, ... Hyman BT (2015). Amyloid accelerates tau propagation and toxicity in a model of early Alzheimer's disease. *Acta Neuropathol Commun*, 3, 14 10.1186/s40478-015-0199-x [PubMed: 25853174]
- Rahimi J, & Kovacs GG (2014). Prevalence of mixed pathologies in the aging brain. *Alzheimers Res Ther*, 6(9), 82 10.1186/s13195-014-0082-1 [PubMed: 25419243]
- Rapp PR, & Amaral DG (1989). Evidence for task-dependent memory dysfunction in the aged monkey. *J Neurosci*, 9(10), 3568–3576. [PubMed: 2795141]
- Rapp PR, Morrison JH, & Roberts JA (2003). Cyclic estrogen replacement improves cognitive function in aged ovariectomized rhesus monkeys. *J Neurosci*, 23(13), 5708–5714. [PubMed: 12843274]
- Rapp SR, Espeland MA, Shumaker SA, Henderson VW, Brunner RL, Manson JE, ... Investigators W (2003). Effect of estrogen plus progestin on global cognitive function in postmenopausal women: the Women's Health Initiative Memory Study: a randomized controlled trial. *JAMA*, 289(20), 2663–2672. 10.1001/jama.289.20.2663 [PubMed: 12771113]

- Regan P, Piers T, Yi JH, Kim DH, Huh S, Park SJ, ... Cho K (2015). Tau phosphorylation at serine 396 residue is required for hippocampal LTD. *J Neurosci*, 35(12), 4804–4812. 10.1523/JNEUROSCI.2842-14.2015 [PubMed: 25810511]
- Regan P, Whitcomb DJ, & Cho K (2016). Physiological and Pathophysiological Implications of Synaptic Tau. *Neuroscientist* 10.1177/1073858416633439
- Reyna-Neyra A, Camacho-Arroyo I, Ferrera P, & Arias C (2002). Estradiol and progesterone modify microtubule associated protein 2 content in the rat hippocampus. *Brain Res Bull*, 58(6), 607–612. [PubMed: 12372566]
- Roberson ED, Halabisky B, Yoo JW, Yao J, Chin J, Yan F, ... Mucke L (2011). Amyloid-beta/Fyn-induced synaptic, network, and cognitive impairments depend on tau levels in multiple mouse models of Alzheimer's disease. *J Neurosci*, 31(2), 700–711. 10.1523/JNEUROSCI.4152-10.2011 [PubMed: 21228179]
- Roberts JA, Gilardi KV, Lasley B, & Rapp PR (1997). Reproductive senescence predicts cognitive decline in aged female monkeys. *Neuroreport*, 8(8), 20472051.
- Rocca WA, Bower JH, Maraganore DM, Ahlskog JE, Grossardt BR, de Andrade M, & Melton LJ, 3rd. (2007). Increased risk of cognitive impairment or dementia in women who underwent oophorectomy before menopause. *Neurology*, 69(11), 1074–1083. 10.1212/01.wnl.0000276984.19542.e6 [PubMed: 17761551]
- Rocca WA, Grossardt BR, & Shuster LT (2011). Oophorectomy, menopause, estrogen treatment, and cognitive aging: clinical evidence for a window of opportunity. *Brain Res*, 1379, 188–198. 10.1016/j.brainres.2010.10.031 [PubMed: 20965156]
- Rosen RF, Farberg AS, Gearing M, Dooyema J, Long PM, Anderson DC, ... Walker LC (2008). Tauopathy with paired helical filaments in an aged chimpanzee. *J Comp Neurol*, 509(3), 259–270. 10.1002/cne.21744 [PubMed: 18481275]
- Ruitenber A, Ott A, van Swieten JC, Hofman A, & Breteler MM (2001). Incidence of dementia: does gender make a difference? *Neurobiol Aging*, 22(4), 575–580. [PubMed: 11445258]
- Ryan J, Scali J, Carriere I, Amieva H, Rouaud O, Berr C, ... Ancelin ML (2014). Impact of a premature menopause on cognitive function in later life. *BJOG*, 121(13), 1729–1739. 10.1111/1471-0528.12828 [PubMed: 24802975]
- Salter MW, & Kalia LV (2004). Src kinases: a hub for NMDA receptor regulation. *Nat Rev Neurosci*, 5(4), 317–328. 10.1038/nrn1368 [PubMed: 15034556]
- Schneider A, Biernat J, von Bergen M, Mandelkow E, & Mandelkow EM (1999). Phosphorylation that detaches tau protein from microtubules (Ser262, Ser214) also protects it against aggregation into Alzheimer paired helical filaments. *Biochemistry*, 38(12), 3549–3558. 10.1021/bi981874p [PubMed: 10090741]
- Schultz C, Hubbard GB, Rub U, Braak E, & Braak H (2000). Age-related progression of tau pathology in brains of baboons. *Neurobiol Aging*, 21(6), 905–912. [PubMed: 11124441]
- Shao H, Breitner JC, Whitmer RA, Wang J, Hayden K, Wengreen H, ... Cache County, I. (2012). Hormone therapy and Alzheimer disease dementia: new findings from the Cache County Study. *Neurology*, 79(18), 1846–1852. 10.1212/WNL.0b013e318271f823 [PubMed: 23100399]
- Shi HR, Zhu LQ, Wang SH, Liu XA, Tian Q, Zhang Q, ... Wang JZ (2008). 17beta-estradiol attenuates glycogen synthase kinase-3beta activation and tau hyperphosphorylation in Akt-independent manner. *J Neural Transm (Vienna)*, 115(6), 879–888. 10.1007/s00702-008-0021-z [PubMed: 18217188]
- Shumaker SA, Legault C, Kuller L, Rapp SR, Thal L, Lane DS, ... Women's Health Initiative Memory, S. (2004). Conjugated equine estrogens and incidence of probable dementia and mild cognitive impairment in postmenopausal women: Women's Health Initiative Memory Study. *JAMA*, 291(24), 2947–2958. 10.1001/jama.291.24.2947 [PubMed: 15213206]
- Shumaker SA, Legault C, Rapp SR, Thal L, Wallace RB, Ockene JK, ... Investigators W (2003). Estrogen plus progestin and the incidence of dementia and mild cognitive impairment in postmenopausal women: the Women's Health Initiative Memory Study: a randomized controlled trial. *JAMA*, 289(20), 2651–2662. 10.1001/jama.289.20.2651 [PubMed: 12771112]

- Sloane JA, Pietropaolo MF, Rosene DL, Moss MB, Peters A, Kemper T, & Abraham CR (1997). Lack of correlation between plaque burden and cognition in the aged monkey. *Acta Neuropathol*, 94(5), 471–478. [PubMed: 9386780]
- Squire LR, Zola-Morgan S, & Chen KS (1988). Human amnesia and animal models of amnesia: performance of amnesic patients on tests designed for the monkey. *Behav Neurosci*, 102(2), 210–221. [PubMed: 3130073]
- Suzuki M, & Kimura T (2017). Microtubule-associated tau contributes to intra-dendritic trafficking of AMPA receptors in multiple ways. *Neurosci Lett*, 653, 276–282. 10.1016/j.neulet.2017.05.056 [PubMed: 28554859]
- Tai HC, Wang BY, Serrano-Pozo A, Frosch MP, Spire-Jones TL, & Hyman BT (2014). Frequent and symmetric deposition of misfolded tau oligomers within presynaptic and postsynaptic terminals in Alzheimer's disease. *Acta Neuropathol Commun*, 2, 146 10.1186/s40478-014-0146-2 [PubMed: 25330988]
- Takizawa C, Thompson PL, van Walssem A, Faure C, & Maier WC (2015). Epidemiological and economic burden of Alzheimer's disease: a systematic literature review of data across Europe and the United States of America. *J Alzheimers Dis*, 43(4), 1271–1284. 10.3233/JAD-141134 [PubMed: 25159675]
- Tigges J, Gordon TP, McClure HM, Hall EC, & Peters A (1988). Survival rate and life span of rhesus monkeys at the Yerkes regional primate research Center. *Am J Primatol*, 15, 263–273.
- Vingtdeux V, Davies P, Dickson DW, & Marambaud P (2011). AMPK is abnormally activated in tangle- and pre-tangle-bearing neurons in Alzheimer's disease and other tauopathies. *Acta Neuropathol*, 121(3), 337–349. 10.1007/s00401-010-0759-x [PubMed: 20957377]
- Voelzmann A, Okenve-Ramos P, Qu Y, Chojnowska-Monga M, Del Cano-Espinel M, Prokop A, & Sanchez-Soriano N (2016). Tau and spectraplakins promote synapse formation and maintenance through Jun kinase and neuronal trafficking. *Elife*, 5 10.7554/eLife.14694
- Voytko ML (2000). The effects of long-term ovariectomy and estrogen replacement therapy on learning and memory in monkeys (*Macaca fascicularis*). *Behav Neurosci*, 114(6), 1078–1087. [PubMed: 11142640]
- Walker ML, & Herndon JG (2008). Menopause in nonhuman primates? *Biol Reprod*, 79(3), 398–406. 10.1095/biolreprod.108.068536 [PubMed: 18495681]
- Wang AC, Hara Y, Janssen WG, Rapp PR, & Morrison JH (2010). Synaptic estrogen receptor-alpha levels in prefrontal cortex in female rhesus monkeys and their correlation with cognitive performance. *J Neurosci*, 30(38), 12770–12776. 10.1523/JNEUROSCI.3192-10.2010 [PubMed: 20861381]
- Wang Y, & Mandelkow E (2016). Tau in physiology and pathology. *Nat Rev Neurosci*, 17(1), 5–21. 10.1038/nrn.2015.1 [PubMed: 26631930]
- Watanabe A, Hasegawa M, Suzuki M, Takio K, Morishima-Kawashima M, Titani K, ... Ihara Y (1993). In vivo phosphorylation sites in fetal and adult rat tau. *J Biol Chem*, 268(34), 25712–25717. [PubMed: 8245007]
- Weingarten MD, Lockwood AH, Hwo SY, & Kirschner MW (1975). A protein factor essential for microtubule assembly. *Proc Natl Acad Sci U S A*, 72(5), 1858–1862. [PubMed: 1057175]
- Whitmer RA, Quesenberry CP, Zhou J, & Yaffe K (2011). Timing of hormone therapy and dementia: the critical window theory revisited. *Ann Neurol*, 69(1), 163–169. 10.1002/ana.22239 [PubMed: 21280086]
- Woller MJ, Everson-Binotto G, Nichols E, Acheson A, Keen KL, Bowers CY, & Terasawa E (2002). Aging-related changes in release of growth hormone and luteinizing hormone in female rhesus monkeys. *J Clin Endocrinol Metab*, 87(11), 5160–5167. 10.1210/jc.2002-020659 [PubMed: 12414887]
- Yague JG, Wang AC, Janssen WG, Hof PR, Garcia-Segura LM, Azcoitia I, & Morrison JH (2008). Aromatase distribution in the monkey temporal neocortex and hippocampus. *Brain Res*, 1209, 115–127. 10.1016/j.brainres.2008.02.061 [PubMed: 18402929]
- Yamauchi PS, & Purich DL (1993). Microtubule-associated protein interactions with actin filaments: evidence for differential behavior of neuronal MAP-2 and tau in the presence of phosphatidyl-

inositol. *Biochem Biophys Res Commun*, 190(3), 710–715. 10.1006/bbrc.1993.1107 [PubMed: 8439322]

Yeow MB, & Peterson EH (1991). Active zone organization and vesicle content scale with bouton size at a vertebrate central synapse. *J Comp Neurol*, 307(3), 475–486. 10.1002/cne.903070310 [PubMed: 1856332]

Zhang Z, & Simpkins JW (2010). Okadaic acid induces tau phosphorylation in SHSY5Y cells in an estrogen-preventable manner. *Brain Res*, 1345, 176–181. 10.1016/j.brainres.2010.04.074 [PubMed: 20457142]

Zheng-Fischhofer Q, Biernat J, Mandelkow EM, Illenberger S, Godemann R, & Mandelkow E (1998). Sequential phosphorylation of Tau by glycogen synthase kinase-3beta and protein kinase A at Thr212 and Ser214 generates the Alzheimer-specific epitope of antibody AT100 and requires a paired-helicalfilament-like conformation. *Eur J Biochem*, 252(3), 542–552. [PubMed: 9546672]

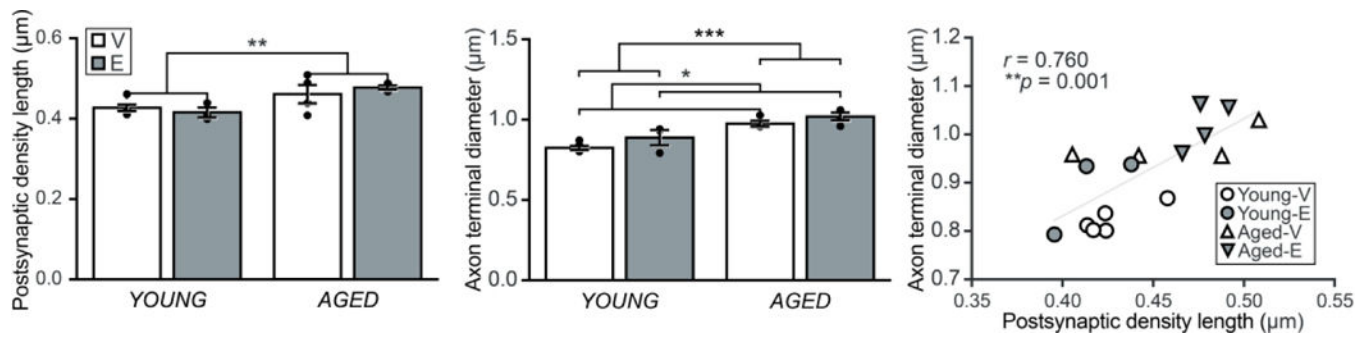


Figure 1.

Synapse morphology. Bar graphs of the average postsynaptic density length (left), and the average axon terminal diameter (middle) across age and treatment groups; and, the positive correlation between postsynaptic density length and axon terminal diameter for each monkey (right). V, vehicle; E, estradiol. Individual data points represent the average value for each monkey. Group results (bars) are expressed as the mean \pm SEM. Young-V, $n = 5$; young-E, $n = 3$; aged-V, $n = 4$; aged-E, $n = 4$ monkeys.

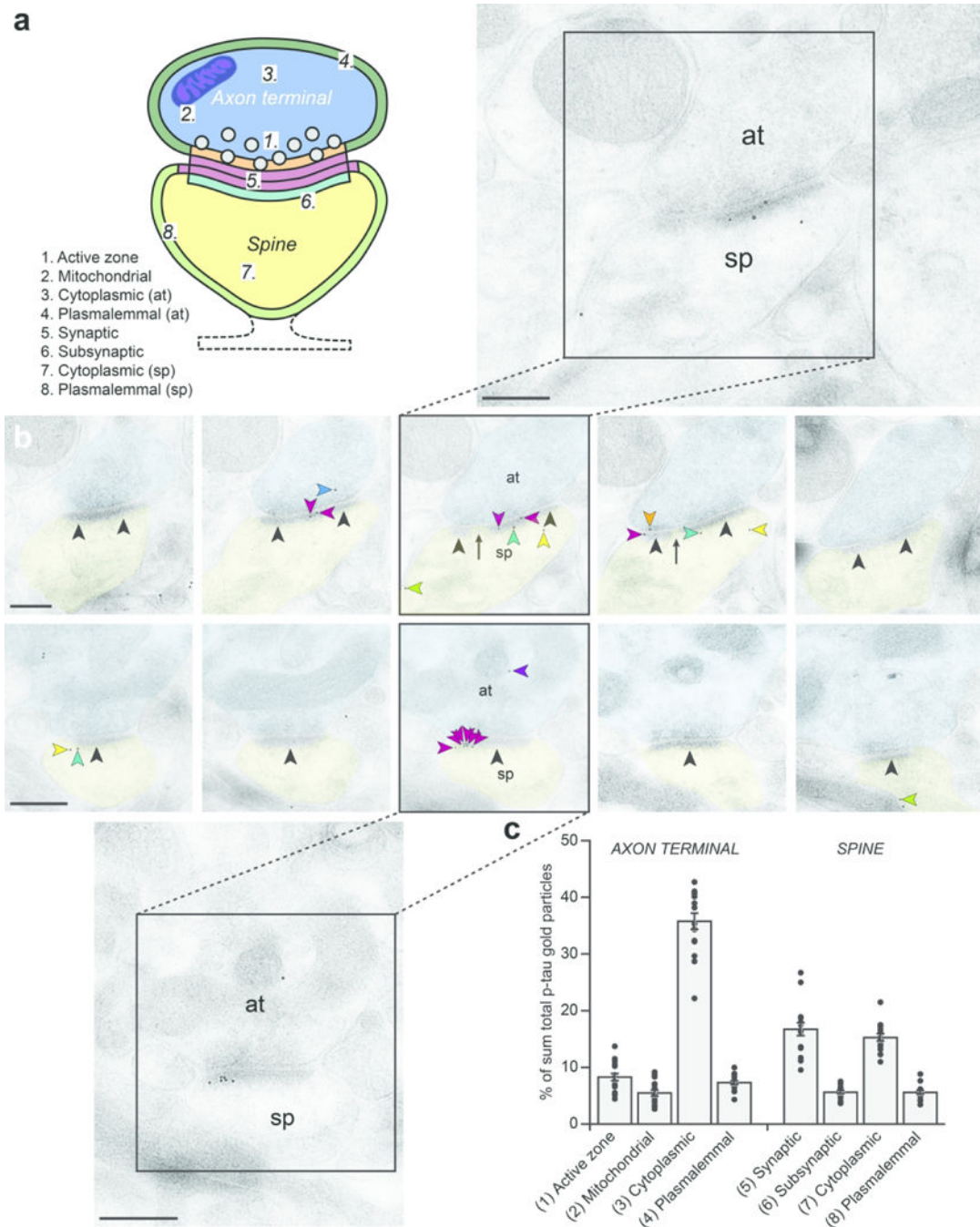


Figure 2. Subcellular synaptic representations of pS214-tau immunogold particles. **(a)** Schematic diagram illustrating the eight domains used to categorize the location of each pS214-tau immunogold particle. **(b)** Representative electron micrographs of five serial sections through a pS214-tau-containing perforated synapse spine (top row), and nonperforated synapse spine (bottom row). The postsynaptic densities are well defined, and easily distinguishable (black arrowheads). Black arrows point to the discontinuity in the postsynaptic density of the perforated synapse spine. pS214-tau immunogold particles (arrowheads) are shown localized

to the presynaptic active zone (orange), mitochondrial (purple), and cytoplasmic (blue) domains; and, postsynaptic synaptic (magenta), subsynaptic (cyan), cytoplasmic (yellow), and plasmalemmal (green) domains. For each series, the third section (outlined with a black box) was used as a reference section, and all synapses containing a dendritic spine that possessed a readily apparent postsynaptic density in this section were marked, and followed throughout the series for subsequent morphological and immunolabeling analyses. Immunogold particles, specifically localized to the synaptic complex, are prominent in expanded versions of reference sections (insets). Scale bars, 250 nm. (c) Bar graph of the percentage of pS214-tau immunogold particles localized to each of the 8 synaptic domains averaged across all monkeys. V, vehicle; E, estradiol. At, axon terminal; sp, dendritic spine. Individual data points represent the average value for each monkey. Group results (bars) are expressed as the mean \pm SEM. Young-V, $n = 5$; young-E, $n = 3$; aged-V, $n = 4$; aged-E, $n = 4$ monkeys.

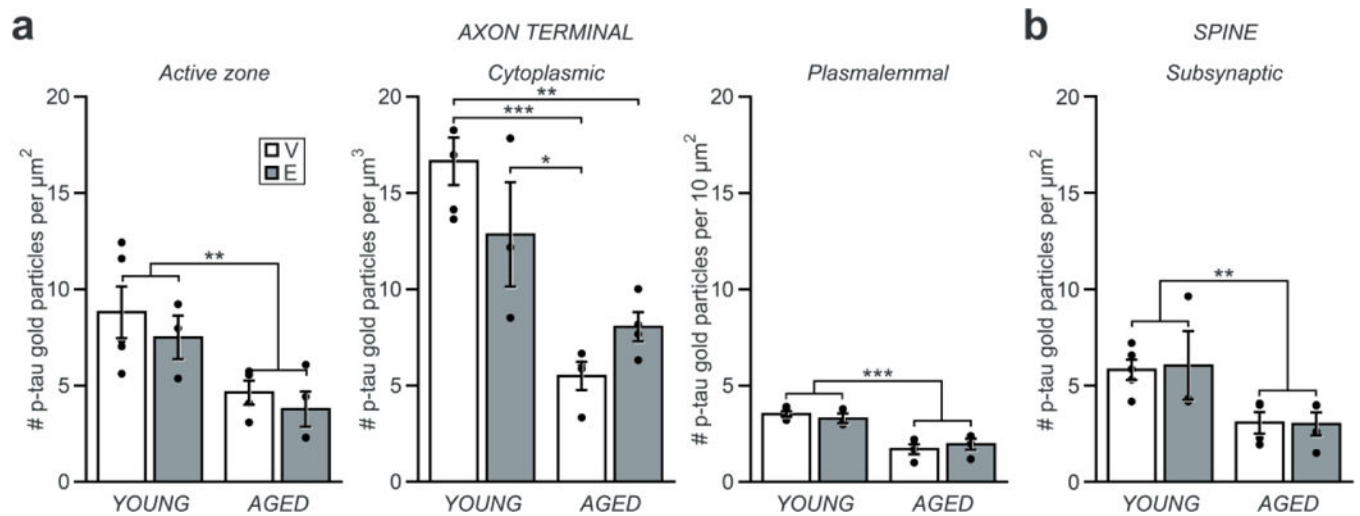


Figure 3.

Density of pS214-tau immunogold particles. **(a)** Bar graphs of the average density of pS214-tau immunogold particles in the active zone (left), cytoplasmic (middle), and plasmalemmal (right) domains of axon terminals. **(b)** Bar graph of the average density of pS214-tau immunogold particles in the subsynaptic domain of dendritic spines. V, vehicle; E, estradiol. Individual data points represent the average value for each monkey. Group results (bars) are expressed as the mean \pm SEM. Young-V, $n = 5$; young-E, $n = 3$; aged-V, $n = 4$; aged-E, $n = 4$ monkeys.

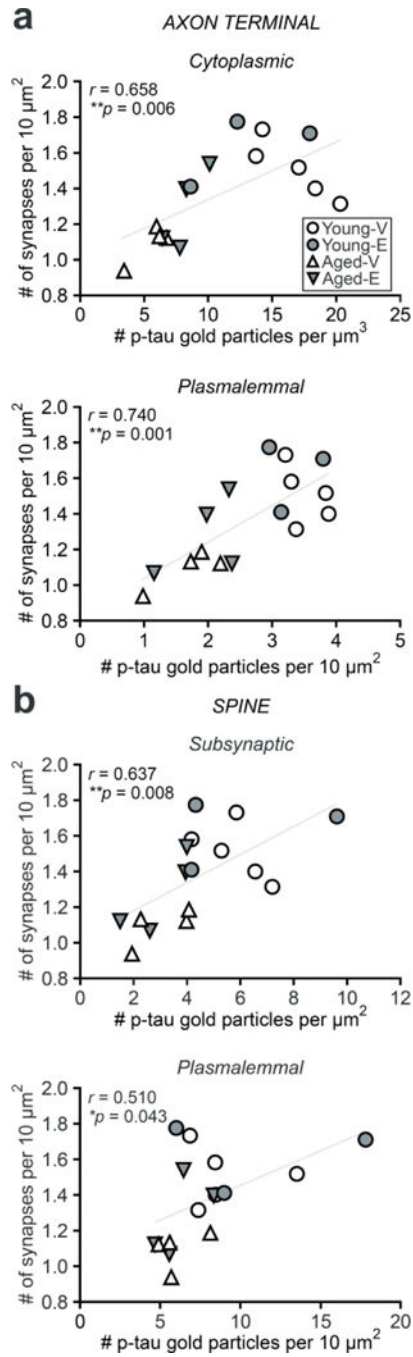


Figure 4. Relationship of the density of pS214-tau immunogold particles to synapse density. **(a)** Positive correlation between the average density of pS214-tau immunogold particles in axon terminal cytoplasmic (top), and plasmalemmal (bottom) domains to synapse density for each monkey. **(b)** Positive correlation between the average density of pS214-tau immunogold particles in dendritic spine subsynaptic (top), and plasmalemmal (bottom) domains to synapse density for each monkey. V, vehicle; E, estradiol.

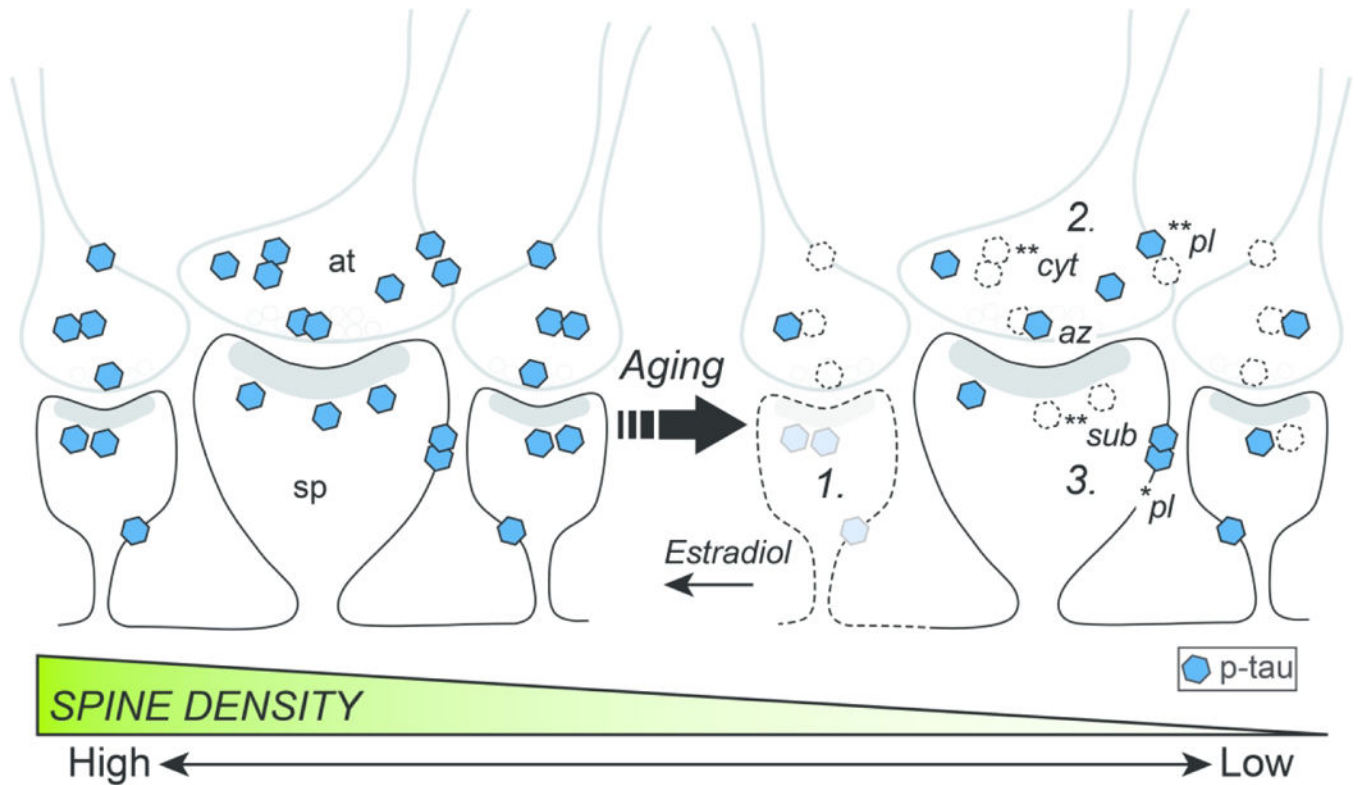


Figure 5. Schematic diagram illustrating proposed relationships of synaptic distributions of pS214-tau to aging, estradiol, and spine density. **(1)** Small synapse spines are lost with age, and are partially restored to levels of young monkeys with estrogen treatment (Crimins et al., 2017; Dumitriu et al., 2010; Hao et al., 2007). **(2)** In axon terminals, pS214-tau is lost from the active zone, cytoplasmic, and plasmalemmal domains with age. **(3)** In dendritic spines, pS214-tau is lost from the subsynaptic domain. Such changes appear to target small and large spine types, and thus are depicted in both synaptic subclasses. Asterisks corresponding to the significance level for each Pearson's correlation indicate domains where lower pS214-tau density strongly couples to synapse loss. At, axon terminal; az, active zone; cyt, cytoplasmic domain; pl, plasmalemmal domain; sp, spine; sub, subsynaptic domain. * $p < 0.05$; ** $p < 0.01$.

Table 1.

DR task acquisition and performance accuracy. V, vehicle; E, estradiol; TTC, trials to criterion; s, second; DR, delayed response. Group results are expressed as the mean \pm SEM. Young-V, $n = 5$; young-E, $n = 3$; aged-V, $n = 4$; aged-E, $n = 4$ monkeys.

	Young-V	Young-E	Aged-V	Aged-E
DR TTC 0-s (# of trials)	227.800 \pm 92.945	192.00 \pm 115.487	315.750 \pm 176.290	68.750 \pm 29.364
DR TTC 1-s (# of trials)	346.000 \pm 216.993	86.667 \pm 67.660	139.500 \pm 69.115	22.500 \pm 16.520
DR 5-s (% correct)	74.880 \pm 3.385	88.167 \pm 2.042	75.275 \pm 2.659	87.800 \pm 3.016
DR 10-s (% correct)	75.100 \pm 3.204	81.467 \pm 10.752	72.500 \pm 1.393	83.350 \pm 6.205
DR 15-s (% correct)	70.920 \pm 5.939	87.000 \pm 6.332	69.175 \pm 4.040	79.425 \pm 8.910
DR 30-s (% correct)	72.000 \pm 6.380	78.867 \pm 13.333	59.475 \pm 2.504	69.425 \pm 5.751
DR 60-s (% correct)	67.880 \pm 9.790	74.100 \pm 9.386	55.575 \pm 2.400	59.175 \pm 2.516
DR average (% correct)	72.156 \pm 5.164	81.920 \pm 8.079	66.400 \pm 1.023	75.835 \pm 4.727